Sacks, I.S., Suyehiro, K., Acton, G.D., et al., 2000
Proceedings of the Ocean Drilling Program, Initial Reports Volume 186

3. Borehole Instrument Package[1]

Shipboard Scientific Party[2]

SYSTEM OVERVIEW

Purpose

The lack of in situ long-term observations in the oceans, which cover areas of major tectonic activity, limits our understanding of presently active geological processes. Since the beginning of the Deep Sea Drilling Project, there have been many attempts to utilize the drilled holes for observatory purposes. Recent circulation obviation retrofit kit deployments (CORKS) to measure pressure and temperature changes in sealed boreholes are beginning to produce interesting results. The Ocean Drilling Program (ODP) continues to recognize the importance of observatory objectives (ODP, 1996).

Many ODP sites have been drilled at plate subduction zones to understand the accretion processes, to tackle the mass balance problems, or to construct the history of the making of island arcs, among other objectives. A major unknown in the plate subduction process is its episodic nature. Our main goal for Leg 186 was to install two permanent observatories on the landward side of the Japan Trench directly above the seismogenic zone of the subduction plate boundary. The two sites, Sites 1150 and 1151, are located in presently seismically active and inactive zones, respectively.

At a plate subduction zone, there is coupling between the two plates, but the definition of coupling can be confusing. One measure is the seismic efficiency, which is the percentage of plate motion released by interplate thrust earthquakes. Plate motion is determined from global plate velocity models. For the Japan Trench zone, the seismic efficiency is probably <~30%. Another measure of coupling is how locked a portion of a plate boundary is relative to adjacent portions. A 100%-locked condition means that there is normally no differential motion across a part of the plate boundary. Eventually slip must occur, the presumption

[1]Examples of how to reference the whole or part of this volume.
[2]Shipboard Scientific Party addresses.

Ms 186IR-103

being that it will be manifest as a sizable earthquake. Since 1994, Global Positioning System (GPS) observations have not revealed any slow earthquakes comparable to or larger than the one that accompanied the 1994 Far-off Sanriku earthquake. The stress transfer across the plate boundary (shear coupling) is a third measure of coupling. In the Japan Trench, the plate motion direction largely governs the tectonic stress field in a wide area across the island arc to the Sea of Japan.

The Japan Trench Borehole Geophysical Observatories provide seismic and deformation data to help quantify these characteristics. The observatory system is named ‘Neath Seafloor Equipment for Recording Earth’s Internal Deformation (NEREID).

NEREID System Outline

This section will outline the borehole geophysical observatory (Fig. F1). Each component is detailed in a separate section. The observatory is designed to last for many years, first as a stand-alone system, then as a system cabled to the shore. Comprised of a strainmeter, a tiltmeter, and two broadband seismometers, the sensors reside near the bottom of the hole with each housed in a separate pressure vessel. Four cables connect the sensors uphole. Except for one seismometer, Guralp Systems Ltd.’s CMG-1T, the signals are sent in analog form. The relative orientation of the sensors is fixed and known. The absolute orientation of the installed systems was not known at installation time but will be determined to sufficient accuracy from the recordings of earthquake waves by the seismometers.

F1. Schematic view of the NEREID borehole geophysical observatory, p. 23.

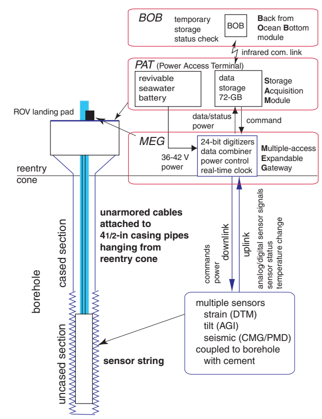

The multiple-access expandable gateway (MEG) seafloor package digitizes and combines the analog-to-digital (A/D) data from downhole to one serial data stream. It also distributes the power to individual modules. The data are stored in digital format in the storage acquisition module (SAM) via an RS232 link using Guralp compressed format (GCF) protocol. The SAM has four 18-GB small computer system interface (SCSI) hard disks equivalent to more than seven channels of 1-yr-long continuous data of 24-bit dynamic range at 100-Hz sampling rate. In this case, there are three channels each for the seismometers (100 Hz for the CMG seismometer and 20 Hz for the PMD seismometer), two channels for the tiltmeter (4 Hz), and nine channels for the three-component and three channels for the single-component strainmeter (50-Hz sampling rate). The borehole sensors are permanently cemented in as required for the strainmeter operation and to assure good coupling for the other sensors. The MEG, on the other hand, may be serviced by a submersible remotely operated vehicle (ROV). The MEG can be physically replaced and accepts commands and software upgrades through the SAM. The SAM needs to be replaced by a submersible ROV before the disks become full, which takes ~1 yr in the present design.

The back from ocean bottom module (BOB) provides a communication link to the borehole system while the station is being serviced by a submersible ROV. The BOB can extract data through the SAM, calibrate the clock, and check the health of the system.

Except for the BOB, all power is supplied by the seawater battery (SWB) system, which can provide ~18 W with more than 300-kWhr capacity. Its source of energy is the magnesium anode, which needs to be replaced once it is consumed by electrolytic dissolution. Replacement of the magnesium anode is also handled by a submersible ROV.

Site Characteristics

The Japan Trench is probably one of the most suitable sites for testing various ideas associated with the episodic nature of plate subduction and its relation to earthquakes and tectonics. Although the seismogenic zone itself cannot be reached by present drilling capability, the present target depth of ~1 km below seafloor provides stations within 10 km of the seismogenic zone of the plate boundary. Since the plate dip angle is very shallow (<10°), a wide area can be viewed by these stations. The nearest geodetic stations are coastal stations ~50 km above the plate boundary; that part of the plate interface may be below the lower-dip end of the seismogenic zone.

Site 1150 and Site 1151 can be considered as two end-members in terms of seismicity. The background seismicity is high around Site 1150 but the area around Site 1151 is aseismic. The former has experienced M7-class events, but there is no historical record of large earthquakes rupturing the area of Site 1151. Although both the microseismicity and large events have contrasting characteristics, there is no compelling evidence of structural differences between the two sites.

For high-sensitivity measurements, pressure fluctuations caused by ocean long waves or temperature changes can be sources of noise, as can water motion near the sensor. Thus the sites are located at key geophysical coordinates and in boreholes for noise reduction. Because of its principle of operation, the strainmeter needs to be grouted inside the borehole to respond accurately to strain changes in the surrounding rock.

INSTALLATION TECHNIQUES

Requirements

A major objective of the installation of the observatories is to monitor the changes in the deformation state of the overlying strata in an active subduction zone. To achieve this, a suitable instrument, described in **"Borehole Instruments,"** p. 5, has to be in intimate contact with the rock. This is accomplished by cementing a resilient instrument in the bottom of an open hole in competent, indurated rock. Although all instruments benefit to some extent by being emplaced in competent rock, this is critical for successful strain monitoring. Depths at least 1 km below seafloor are generally required in areas with thick sediment cover.

One complication of subseafloor installations results from having to cope with irreducible ship heave during hole entry. Since heave can be 1 m or more, cables linking the instruments with the seafloor data handling units have to be protected from stresses created by the relative motion between the cables and the hole wall and between the cables and any insertion tools. Even though the heave compensator is used during hole entry, the instrument string has to hang from the rig floor with no compensation while pipe is being added, and this is repeated every 10–30 m for more than 1 km of hole penetration.

In addition, in order for the cement to set up properly, the instrument package has to be completely undisturbed for ~1 day after the cement is introduced.

Method

The technique we developed to satisfy the installation requirements is illustrated in Figure F2. The instrument package is supported on 4½-in diameter casing pipe that hangs on the base of the reentry cone at the seafloor. This has two advantages: (1) the pipe provides a conduit for cement pumping, and (2) it also keeps the package stationary once its support (riser/casing hanger) lands on the hanger at the base of the cone. After cementing, the drill pipe from the ship can be uncoupled and withdrawn leaving the casing pipe in the hole. The cables are protected by being strapped to the casing pipe and also are protected from wall contact by centralizers (Fig. F77, p. 158, in the "Site 1150" chapter); therefore there is no motion between the cables and the support tube (casing pipe) and no contact with the borehole walls. Strapping the cables to the support tube minimizes the tension in the cables. Armored cables are not required, and the cable structure is almost neutrally buoyant in seawater, further minimizing the long-term stress on the cables.

Cement pumped through a pipe into a water-filled hole does not penetrate much below the pipe opening, tending rather to force its way upward. On land it is possible to have a clean hole down to the bottom and to place a grout slug down on the bottom. This is optimum. In seafloor holes it is impossible to clear all the cuttings from the bottom of the hole. In Hole 1150D, for example, the bottom 7 m was found to be filled with detritus when checked with a wiper trip. In addition, the bottom of the cement column could be diluted and have rather poor strength. To make a strong plug below the instrument, an ~3-m-long extension tube called a "stinger" is coupled to the bottom of the strainmeter. This ensures that the strainmeter is sealed off from the bottom of the hole and that a strong cement plug extends well below the instrument.

The cement is pumped through the casing pipe, the coupling tube, the strainmeter, and the stinger, and then up around the instrument string and into the 10¾-in casing. In Hole 1150D the open hole was 105 m, and the end of the stinger was 17 m above the bottom of the hole. Cement was pumped through the bottom of the stinger, filling ~150 m of the hole.

The amount of cement fill has to be a compromise. Since the cement density is ~2000 kg/m^3, a column of cement will cause an overpressure at the position of the instruments. This is desirable because it will tend to close microfractures and also be forced into cracks in the formation; however, too much overpressure causes hydrofracturing. Maximum pressure estimation requires knowledge of the tensile strength of the rock as well as of the pore pressure. Since neither is known well enough to make the calculation reliable, we adopted a conservative value of 150 m.

Figure F3 is a schematic of instrument installation. Each of the four sensors has its own cable to the seafloor unit. There are several reasons why this plan has been adopted rather than having a single armored cable carrying all the signals. Since we do not know the exact installation depth until the hole has been drilled and the formation evaluated, the downhole cable cannot be cut and terminated ahead of time. Cable termination with an underwater mateable connector (UMC) is a critical operation and takes ~12 hr for four connectors. With the flexible cable used, enough slack can be provided so that errors in the termination operation can be corrected. With armored cable this would be impossi-

F2. Instrument installation technique, p. 24.

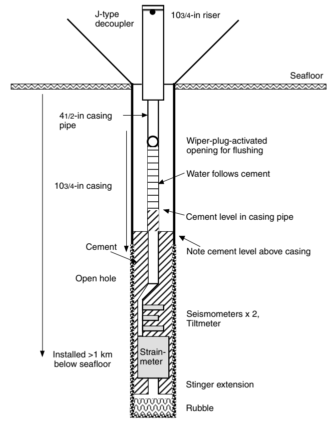

F3. Schematic of the instrument environment at Hole 1151B, p. 25.

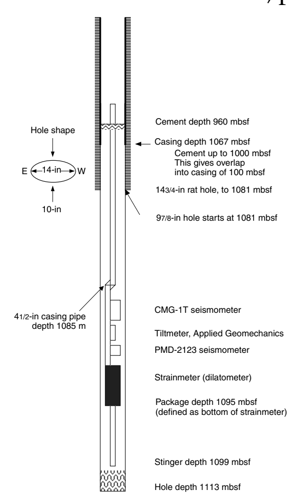

ble and the termination would be extremely difficult to accomplish on the ship. Since some of the signals are noisy digital and others are low-level analog, multiple cables give minimum cross talk in the >1-km-long shared path.

An overriding concern has been the longevity of the installation. A 10-yr goal is necessary to achieve all of the scientific objectives. Our experience with long-lived on-land installations is that cable leakage and electronic component failure are the most likely sources of data termination. For this reason we use multiple cables and much of the electronic circuitry is in a seafloor removable unit, described in "Seafloor Instruments," p. 11.

BOREHOLE INSTRUMENTS

Strainmeter

At the two sites, we deployed two different borehole strainmeters, both modifications of the original Sacks-Evertson (Sacks et al., 1971) design. Instruments of the original design have provided critical deformation data for studies of slow earthquakes (e.g., Sacks et al., 1981; Linde et al., 1988; Linde et al., 1996) and revealed new detail in volcanic activity (Linde et al., 1993; Linde et al., 1994). We installed a three-component strainmeter at Site 1150 and a single-component (dilatometer) version at Site 1151. This section will describe these designs as well as the electronic control system and signal conditioning that provides the analog signals for the A/D converters.

Dilatometer Design

The dilatometer, which measures a single component (dilatation) of strain, resembles the Sacks-Evertson strainmeter. Figure F4 illustrates its basic principle of operation. The sensing volume is filled with a liquid (silicone oil). As the cylinder is deformed, oil is forced in or out of the attached bellows; the top surface of the bellows (B) correspondingly moves up or down. That motion is monitored by a differential transformer (DT). For a given strain, the bellows moves a distance proportional to the sensing volume divided by the bellows cross-sectional area. That ratio is very large (~40,000) and so the instrument provides high hydraulic (noise free) gain. This results in the instrument's having great sensitivity. To keep the strainmeter within its operating range over indefinite time intervals, a valve is opened for a few seconds as needed to allow oil to flow to or from a reservoir (R) that is decoupled from the strain field.

For installation into seafloor boreholes, significant modifications were required (Fig. F5). As before, strain changes are averaged over the 10-ft-long sensing section, providing considerable advantage over other designs that typically monitor a length of ~10–15 cm. The instrument was designed to operate at the bottom of a 1½-km hole drilled in the ocean bottom under 3 km of water. For this high-pressure environment, we require walls ¾ in (19 mm) thick for an instrument diameter of 8 in (20 cm). Pressure testing verified that the dilatometer is capable of operating at pressures of up to 9000 psi (60 MPa). The actual pressure at installation time was ~6000 psi (40 MPa). The installation procedure (see "Installation Techniques," p. 3) requires that cement be pumped through the strainmeter. An off-center cylinder (2¾-in diameter, ⅜-in

F4. Schematic representation of the basic principles for the Sacks-Evertson strainmeter, p. 26.

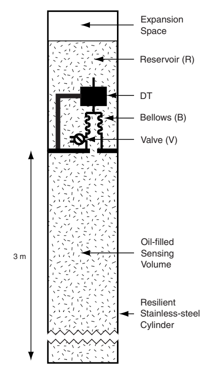

F5. Schematic diagram for the dilatometer deployed in this experiment, p. 27.

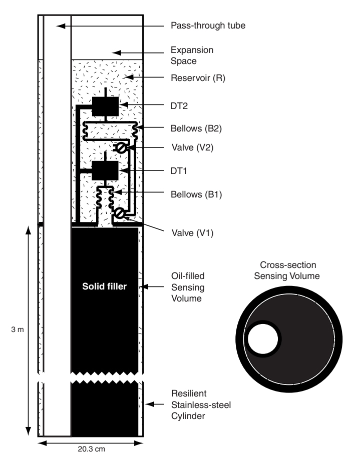

wall thickness) allows this while retaining space for the DT-B subsystems.

The primary signal for strain changes is from a DT (DT1) monitoring the position of a ¾-in-diameter bellows (B1). The B1-DT1 subunit frequency response to strain is constant from 0 to >10 Hz. The sensitivity is ~10^{-12} in strain with a maximum range of ~10^{-5}. In operation, we expect strain changes greater than that maximum. The design allows for larger changes by incorporating a valve (V1) controlled by the electronic package. When V1 is opened, oil flows from or into the sensing volume allowing B1 to return to the equilibrium position. The combination of V1-B1-DT1 was the complete subunit for monitoring the strain changes in the original Sacks-Evertson design. We expect that the instrument will experience a long-term strain rate so that B1 will continue to move slowly away from the equilibrium position. Both to preserve dynamic range for short-term excursions and to obtain lower noise performance, we maintain the bellows close to equilibrium. If the B1 signal level is >15% of its range continuously for more than 15 min, the electronic control unit (Fig. **F5;** see **"Electronic Control and Signal Conditioning,"** p. 8) will open V1 and then close it again 10 s later. Because the instrument response remains constant over the seismic frequency range (order of hertz), the bellows experiences the strain changes caused by seismic waves. For large or nearby earthquakes, as will occur in the vicinity of Sites 1150 and 1151, such strain changes may exceed the maximum range of B1. The electronic control unit (Fig. **F6;** see **"Electronic Control and Signal Conditioning,"** p. 8) continuously checks that B1 is in a safe operating range. If the strain level becomes >60% maximum, V1 is immediately opened to prevent damage. Since this may happen when an earthquake occurs that is important to our program, we could lose valuable data while the valve is open (for ~10 min in this case). We avoid such data loss by incorporating a second monitoring subunit. The exit port from V1 does not connect directly to the oil reservoir but, rather, to a second, larger-diameter bellows (B2). The position of that 2-in-diameter bellows is monitored by a second DT (DT2); a second valve (V2) allows oil to flow between B2 and the unstressed reservoir (R). Whenever V1 is opened and closed, V2 will subsequently be opened after a delay of either 2 hr (following a low-threshold V1 trigger) or 8 hr (following the high-level trigger). Additionally, the output from DT2 is continuously checked and it is kept close to its equilibrium position using the same logic as for DT1. During normal operation the control system does not allow both valves to be open at the same time. Thus the sensing volume is always closed from the reservoir so that we are constantly recording the strain changes. Of course, when V1 is open the sensitivity is reduced by a factor of ~7. Under the common open condition (exceeding the low threshold for 15 min), there is normally no substantial change in the strain condition; only during the emergency high-level condition are we likely to have significant strain changes. But having a temporary gain decrease is of no real concern since the primary sensitivity is so high. When both valves are closed (the usual state during operation), B2-DT2 is monitoring the volume of a fixed mass of oil which is decoupled from the Earth's strain field. DT2 output then gives a measure of temperature change at the installation depth. The system parameters are such that we have a temperature change sensitivity of ~10^{-5}°C.

F6. Block diagram of the strainmeter control electronics, p. 28.

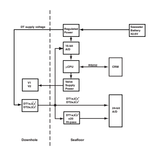

Three-Component Design

The three-component instrument installed at Site 1150 operates using the same hydraulic principle employed in the single-component instrument but incorporates three separate sensing volumes. A schematic illustration (Fig. F7) shows a cross section of the sensing portion that consists of an inner (¾ in thick) and an outer (⅝ in thick) wall with the annulus between them being divided into three equal segments. The objective is to measure, in effect, changes in three diameters (at 120°) of the cylinder, which allows us to record shear changes as well as areal or volume changes. Because the instrument is not circularly symmetric, we have made finite element calculations to verify that nonsymmetry in the design does not introduce significant error into the measurements. As with the high-pressure dilatometer design, this instrument was pressure tested up to 9000 psi to ensure that it could operate under installation conditions. The sensing length is 10 ft and the diameter is 8 in, the same as for the dilatometer. Apart from having three sensing volumes rather than one, the operation of this strainmeter is the same as for the dilatometer. Connected to each oil-filled sensing volume is a monitoring subunit identical to the B1-DT1-V1 combination in the dilatometer. The exit port connects to a second monitoring subunit, again identical to that in the dilatometer. Opening and closing of the valves occurs under the same conditions as in the single-component design, but now there are three sets of signals to monitor. If any of the three primary DTs (DT1a, DT1b, and DT1c) exceeds a threshold condition, all three primary valves (V1a, V1b, and V1c) are opened and then closed again. The secondary valves (V2a, V2b, and V2c) also operate in parallel. This strainmeter also provides high sensitivity and very broadband frequency response. Again, both sets of valves are normally closed during operation, and the second set of DTs gives a sensitive measure of downhole temperature change.

F7. Schematic diagram for the three-component strainmeter, p. 29.

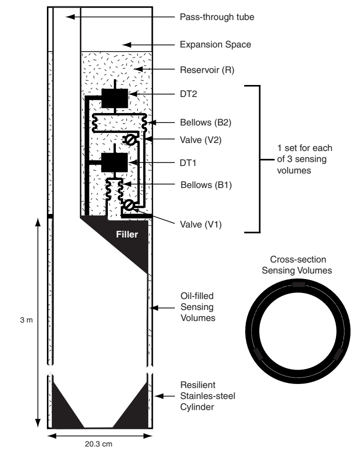

Connection to the Earth

The strainmeters must be bonded well to the host medium to provide meaningful information about changes in the strain state. Prior to the deployment of the original Sacks-Evertson strainmeter, the typical technique employed was to make the connection by means of a mechanical clamping system. Such systems had the advantage that the instrument could be unclamped and retrieved for repair in the event of instrument malfunction. But this came at the expense of instability in the recorded data; such mechanical systems are unable to maintain contact with the surroundings at the level of stability required for good quality data. The technique adopted for the Sacks-Evertson design sacrificed the retrieval capability to preserve the data quality. In all previous cases for installation on land we have used an expansive grout to make the connection between the instrument and the surrounding rock. A quantity of grout was lowered into the hole with a container that opened on reaching the bottom of the hole. After withdrawing that container, the strainmeter was lowered into the hole and sunk through the grout to be completely immersed. As the cement cured, it expanded and locked the instrument to the rock. Thus, the strainmeter subsequently was able to follow strain variations faithfully in the surrounding rock.

For this ocean-bottom installation that procedure must be modified. Sending the cement into the hole first is not feasible. The instrument system is designed to allow cement to be pumped through the instrument assembly and out below it and then fill to above the sensors. Because the strainmeter is already prestressed by the high pressure, it responds to variations in strain in the surroundings without the use of an expansive grout. Tests of the standard cement mixture used for grouting casing in the ODP have verified that its properties are suitable for connecting the strainmeter to the rock.

Electronic Control and Signal Conditioning

The strainmeters are operated and controlled by an electronic unit powered by the seawater battery, which provides a 42.6-V supply. A regulated voltage supply of 6.8 V powers the DTs in the single-component instrument. For the three-component version, all six DTs are powered in parallel (because of the limit to the number of conductors in the cable). We use a regulated supply voltage of 12 V, which is again regulated to 6.8 V in the instrument to eliminate cross talk generated by voltage drop in the 1100-m-long cable (resistance = 16 Ω/km). The outputs of the DTs (the strain signals) are sampled at 20 samples per second (sps) by a multiplexed 16-bit A/D converter. Those digitized data are monitored by a microprocessor that is programmed to send commands to open and close the valves when the threshold conditions are met (see **"Dilatometer Design,"** p. 5). A potential divider provides to the A/D converter an input of one-tenth the supply voltage. If the supply voltage falls below 24 V, indicating failure of the power supply unit, the valves are opened to protect the strainmeter. A capacitor across the input to the electronics has sufficient capacity to allow this protection even if the voltage supply is disconnected.

The strain signals are also sent to amplifiers that provide inputs to the 24-bit A/D converter modules (see **"DM24,"** p. 11). The DT1 and DT2 signals have unity gain amplifiers so that the signal is always within the input voltage range of the digitizers. But a single 24-bit converter (which has ~2 bits of noise) does not cover the complete range of the strainmeter, particularly for the higher frequencies where earth noise is low. We also provide an amplified (20 × gain) output of the DT1 signals. This signal is high-pass filtered with a 3-dB corner frequency of 0.83 mHz (20-min period), which gives the high gain for the higher frequencies and also minimizes saturating the A/D converters as a result of long-period changes.

Ocean Borehole Seismometer

The ocean borehole seismometer (OBHS) is a package consisting of a three-component seismometer and a 24-bit digitizer (DM24) assembled in a stainless-steel pressure cylinder 1 m long with a 12.7-cm outside diameter. The seismometer is model CMG-1T made by Guralp Systems, Ltd., which consists of three orthogonal sensors, stacked vertically in the canister with a vertical sensor above the two horizontal sensors (Fig. **F8**).

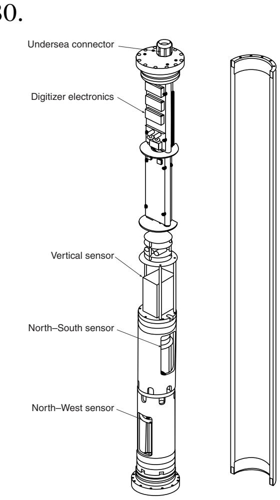

F8. Outline drawing showing the OBHS components in the canister, p. 30.

The OBHS vertical sensor is a modified Lacoste type, and the horizontal sensor is an inverted pendulum. The inertial mass is a boom (a solid machined beam) supporting a transducer coil. The vertical sensor mass is supported by a prestressed triangular spring to support its weight and has a natural period of ~0.5 s. The horizontal sensor mass is centered by an unstressed flat triangular spring and has a natural period of ~1 s. The effective mass of each sensor is ~180 g. The springs are connected to the frames with a temperature compensating wire that minimizes the effect of temperature variation. A compact design is achieved chiefly by the short stiff springs and short boom.

The adjustments required for operation consist of leveling the boom of the vertical sensor and tilting the bases of the horizontal sensors to center the mass movements in their equilibrium positions. These are made by small (1 cm in diameter and 3 cm long) direct current (DC) motors operating gear mechanisms to tilt the horizontal sensor bases and to apply a small extra force to the vertical sensor's boom.

Before and during the installation in the borehole, the instrument may be subjected to severe motion that can damage the mass support hinges. The masses must be locked securely in their frames so that the hinges can be released. This operation is performed by a small motor-driven clamp, which is controlled by a command to the DM24.

The sensors employ feedback to expand their bandwidth and dynamic range. The sensor's response is determined by the characteristics of the feedback loop. The mass position is sensed by the capacitative position sensor. The voltage from the sensor, which is proportional to the displacement of the mass from its equilibrium position, is amplified and fed to a coil on the mass. The current in the coil forces the mass to its equilibrium position. With a high loop gain, motion of the mass is essentially prevented; the feedback voltage is then a measure of the force and, thus, the acceleration applied to the mass. The block diagram of the feedback system is shown in Figure F9. The system velocity response is identical to that of a conventional long-period sensor with a velocity transducer whose natural resonant period is 360 s with a damping factor of 0.707. The velocity output (flat to 100 Hz) is low-pass filtered (<50 Hz) before digitization. The mass position output can be used for periods longer than 360 s.

F9. Schematic diagram for the electronics circuits of the CMG-1T sensors, p. 31.

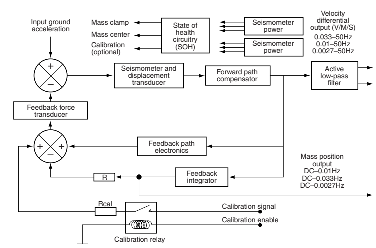

The output signals are digitized by the DM24. The detailed description of the DM24 module is given in **"Seafloor Instruments,"** p. 11. The velocity outputs are digitized at 100 sps, and the mass position outputs at 4 sps. The DM24 also digitizes the signal from the temperature sensor in the OBHS cylinder. All digital data are sent to the MEG through a 1.1-km-long cable. The communication link to the MEG is a four-wire RS422 serial link at 9600 bits per second (bps). As well as sending the signal data, the DM24 receives the time reference signals from the MEG and synchronizes the OBHS clock to the reference; this clock stamps the time in the digitized records.

The microprocessor in DM24 performs various controls of the sensors, such as unlocking/locking of the masses and bases of the horizontal sensors, and centering the masses. These controls are initiated by a command sent from the MEG or autonomously by the OBHS system. The masses are recentered whenever they deviate from the center position by more than half the range of travel.

PMD Seismometer

The PMD seismometer is a three-component seismometer having a fairly broad frequency band response. This unit is a PMD model 2123 repackaged for borehole use. The amplitude response is essentially flat from 25 to 0.03 Hz with useful output down to 0.01 Hz.

The PMD seismometer sensors are robust and require no leveling or clamping. This makes them particularly suitable for borehole installations. The inertial component is a liquid—water with potassium iodide in solution—in a container which includes permeable grids that serve as cathode and anode. Between the grids a small bias voltage (<0.7 V) is applied, resulting in an ion current. Vibration of the instrument produces changes in the motion of the ionized liquid through the electrodes, resulting in a modulation of the ion current. These modulations are the output signal of the seismometer.

A prototype tested at the Nokogiriyama test borehole southeast of Tokyo had a power spectral density noise level [$(m/s^2)^2/Hz$] of about –150 dB at frequencies between 30 and 10 mHz. This is ~13 dB higher than for a CMG-1T unit (see "Ocean Borehole Seismometer," p. 8) in the same borehole. Note that the Nokogiriyama site is not particularly quiet because it is only ~1 km from Tokyo Bay. The noise threshold of the PMD seismometer is probably reliable, but the site noise is 20 dB or more above the CMG-1T threshold. At frequencies >10 mHz, PMD seismometer noise is probably close to the expected ground noise. Below 30 mHz, the performance deteriorates. Figure F10 shows a comparison of PMD seismometer and CMG-1T noise spectra.

F10. Comparison of seismometer noise for the PMD and CMG, p. 32.

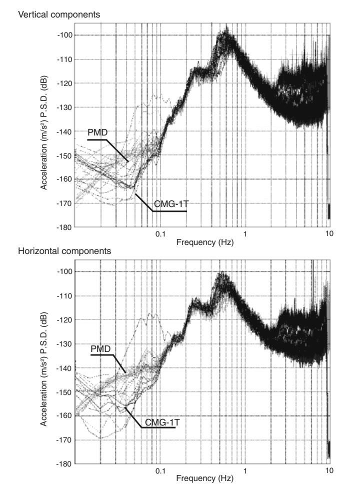

The reason for including a second broad-band seismometer with slightly inferior performance to the primary unit (CMG-1T) is the requirement for a long service life. Although it is impossible to predict the lifetime and failure rate of any complicated mechanism given similar quality and quality control, it is reasonable to expect that the PMD seismometer device with fewer components and moving parts will have a longer life.

Tiltmeter

The tiltmeter is the model 510 developed by Applied Geomechanics. The instrument employs two orthogonal electrolytic tilt sensors to provide the complete tilt vector change as a function of time. We will operate the instrument at maximum sensitivity to provide tilt resolution <10 nanorad with a maximum of 14 microrad. The principle of operation is illustrated in Figure F11. The sensor consists of a conductive fluid and an air bubble inside a curved tube. Excitation electrodes supply alternating current excitation and a pickup electrode provides the output signal. As the sensor tilts, the bubble moves relative to the electrodes and the sensor behaves as a variable resistor. The design is such that the output signal varies linearly with the applied tilt. The sensors and associated electronics are mounted in a vertical cylinder in a housing pressure tested at 7000 psi, well above the operating pressure for our sites.

F11. A schematic representation of the principle of operation of the tilt sensors, p. 33.

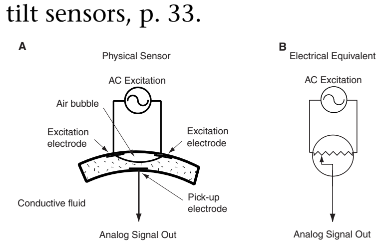

Installing the tiltmeter so that the cylinder is vertical is infeasible, particularly in this below-seafloor installation, and we need a provision to keep the sensors on scale in case of large tilt changes during the instrument's operation. Thus each sensor is mounted on a platform that can be leveled by means of an electric motor. In our installation procedure, the tiltmeter may be subjected to large accelerations, particularly when the instrument string strikes the reentry cone. These tiltmeters have been specially equipped with rugged versions of the leveling units so that they will not be damaged mechanically during installation.

Included in the electronic unit mounted at the ocean bottom is circuitry to provide the signals necessary to drive the leveling motors. This circuitry is controlled by a microprocessor that uses the digitized signal output from a 16-bit A/D to determine which way to drive the leveling motors. The leveling operation will take place at initial system power-up and, subsequently, whenever the tilt sensors move away from the zero position by >40% of the range. The recorded data will come from the 16-bit A/D and the signals will be sampled at 4 sps.

Figure F12 shows ~10 days of data from a similar tiltmeter we installed previously at Nokogiriyama (southeast of Tokyo). Tidal signals are clearly recorded.

Orientations of the Sensors

The orientation of each component of the different sensors is to be estimated from seismometer records of known origin.

SEAFLOOR INSTRUMENTS

MEG

The multiple-access expandable gateway (MEG) is composed of a combiner/repeater module (CRM), A/D converter modules (DM24), a strainmeter interface module, and a PDM seismometer (Fig. F13). The major roles of the MEG are to acquire signals from each sensor, and, for analog sensors, to convert their analog signals to digital data and send out the converted digital data to the SAM via a single serial link, together with an accurate time stamp.

Mechanical Design of the MEG/Frame

All electrical components are stored in an 8.5-in outside-diameter 316 stainless steel canister (Fig. F14). A titanium UMC from Ocean Design, Inc., is installed on its top bulkhead. The UMC is an interface to the SAM and the SWB and is joined by a 20-ft-long oil-filled cable to the power supply access terminal (PAT). On the bottom bulkhead, four stainless-steel Ocean Design, Inc., UMCs are connected to the long cables to the downhole sensors. The MEG frame is a part of the riser pipe assembly that stands in the center of the reentry cone. The MEG can be removed from the frame by pulling up on a rope attached to eyebolts on its top. Thus the MEG is a replaceable component on the seafloor. Two stainless-steel pins are attached each to the top and bottom of the canister to guide the MEG into the frame and to mate the connectors smoothly. The UMCs, whose conductor pins have their own ejecting force, are mated by the >100-kg weight of the MEG in water.

DM24

The DM24 is a modular intelligent digitizer (Fig. F15) developed by Guralp Systems, Ltd. Each DM24 has three single-ended analog input channels to 24-bit A/D converters as well as additional three-component 16-bit A/D channels. Every DM24 consists of five stacked circular printed circuit boards (PCBs) in the MEG, or rectangular PCBs in the OBHS. The 24-bit digitizer utilizes the Crystal Semiconductor (CS) 5321/2 chipset and Motorola 56002 digital signal processor (DSP). The CS5321/2 digitizes the signal at 2000 sps, and the data are processed by the 56002 DSP to give lower sample-rate data. The high sample-rate data are filtered and decimated in four cascaded stages. The first stage decimates the data by 10 to give 200 sps. The following three stages can individually have various decimation factors that allow multiple data output rates to be selected simultaneously. The sampling by CS5321/2 is triggered by a Hitachi H8 16-bit microprocessor. The H8 processor

F12. Tiltmeter data from the Nokogiriyama test site, p. 34.

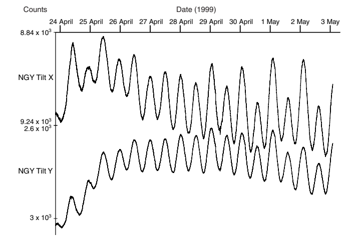

F13. MEG system block diagram, p. 35.

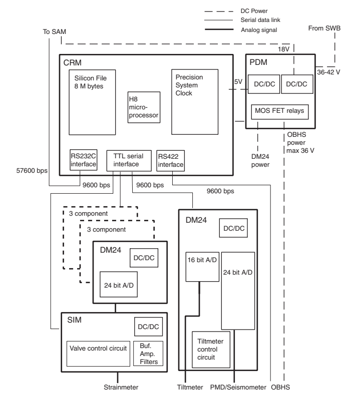

F14. Photograph showing the MEG canister installed in the MEG frame just before they are sent to the seafloor, p. 36.

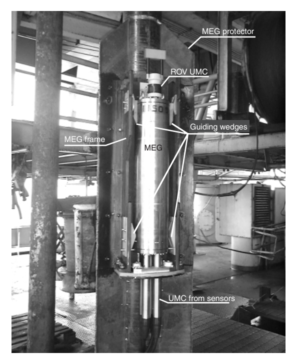

F15. Schematic diagram of the DM24, p. 37.

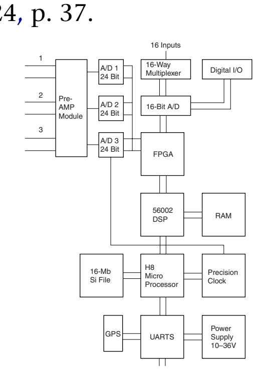

receives data from the DSP, buffers it in 512 KB of static random access memory, and sends it through the serial link to the outside module in GCF. If a packet is lost during data transmission, it can be recovered from the receiver side by a procedure called "block recovery protocol."

GCF, used in transferring data throughout the system, enables sharing of a single transmission line by many different time series data channels. It also incorporates status messages in American Standard Code for Information Interchange (ASCII) characters. Each data transmission in GCF is a packet containing either a data block or a status block. The GCF packet consists of an identification character, transmission serial identification (ID), data/status block contents, and 2-byte checksum characters. The transmission serial ID increases by 1 every packet. Serial numbering enables a receiver to detect loss of a GCF packet, which will result in a request to resend the lost packet. Each data block comprises data in multiples of a full second starting on an exact second. The data block consists of a block header and a compressed data block. The basic attributes of the data (e.g., system ID, stream ID, date and time of the observation data, number of samples per second, number of data in the block, and type of compression in the data block that follows) are stored in a block header. The set of system ID and stream ID identifies the source of the data. The assignment of the system ID/stream ID to each source is listed in Table T1. The data are compressed by recording the first and last complete values in each block and the difference values between adjacent samples. The bit lengths of the difference values are all the same in a data block and are 8, 16, or 32 bits depending on the maximum first difference in the signal in that data block. The status block has the same block header as that of data blocks but is identified by a sps field of 0 and a compression-byte value of 4. After the block header, status information in ASCII characters follows and is terminated by a NUL character. The status block transfers many different types of information such as boot messages, progress reports of seismometer mass control, and measurements of clock offset between that of the CRM and of the DM24s.

T1. GCF mapping between sensor channels and stream ID, p. 50.

The H8 processor also controls the DM24 real-time clock (RTC), which has battery backup power. The processor receives an external time reference signal through the serial link and synchronizes the internal RTC to the reference. The external time reference can be either a GPS or "Stream Sync" time base signal. But in this case all the DM24s in the MEG and the OBHS are configured to use the Stream Sync signal, a set of clock synchronization characters sent by an upstream module through the serial data link of the DM24. The signal consists of 2-byte characters sent every second that encode date and time information over a 1-min sequence. The advantage of the Stream Sync is that it can utilize a low band-width link such as 9600 bps, which is the link speed between all the DM24s and CRM.

Each DM24 has a clock that stamps time on the data sent to CRM. These less-accurate clocks are separate from the precision clock in CRM, which is the master clock for the whole system. Thus, the clock in DM24 must always be synchronized to the master clock in CRM.

DM24s receive the time reference signal and trim their clock oscillators to synchronize with the reference. The measurement of the clock offset and the trimming is made once a minute. The mechanism typically keeps the clock offset between CRM master clock and these slave clocks within 1 ms. DM24s also report the clock offset in units of $1/120$ ms in the status block.

Another DM24 feature is that it is interactively configured or commanded through the same serial link that is used for the data transmission. With a simple command line, control of the sensor attached to the DM24 is possible, such as mass unlock/lock or mass centering of the OBHS. Also, some of the DM24s can have a task that automates the control of the sensors. For example, the DM24 for the CMG-1T seismometer has a process to monitor the mass positions and centers the masses when they deviate by more than half the full scale from the zero position.

Analog signals from the strainmeter are digitized by the DM24 with 24-bit resolution. Nine channels from three DM24 modules are employed for the three-component strainmeter, whereas three channels of a single DM24 are used to digitize the single-component strainmeter. The PMD seismometer and the tiltmeter share a common DM24. The PMD seismometer channels are attached to the 24-bit digitizers, and the two-component tiltmeter signals are connected to 16-bit digitizers. The DM24 dedicated to the PMD seismometer and the tiltmeter differs from the others in that it has three extra circuit boards and a system process to control motors to level the tiltmeter sensors.

Combiner/Repeater Module

The CRM takes digital data from all the DM24s. Serial links between the CRM and the DM24s in the MEG are transistor-transistor logic level interfaces to minimize power consumption of the MEG's line driver/receivers. An RS422 serial interface is used between the CRM and OBHS to ensure a link of sufficient quality over a 1-km-long cable. The data collected by these serial interfaces are handled by a Hitachi H8 microprocessor, buffered sequentially in an 8-MB silicon file and transmitted to the SAM through a high-speed (57600 bps) RS232C serial interface.

The H8 processor controls its precision master RTC in the same manner as for the DM24 RTC. The master RTC is a temperature-compensated precision clock, and the trimming of the oscillator by the processor results in an accuracy exceeding 10^{-8}. Absolute time of the master RTC can be set by sending a stream sync signal from a surface ship via an ROV-BOB connection (see **"BOB,"** p. 16).

On power-up of the system (e.g., when the SWB is connected to the MEG) the CRM begins executing the system program. The CRM also allows the system program to be reloaded from the high-speed serial link. After 20 min of standby time to assure a complete cable connection by the ROV, the CRM begins to handle data transmission and powers up all the DM24s and the sensors sequentially. The power-up sequence of the sensors is as follows:

1. Switch on the SAM and monitor all units for 2 min.
2. Switch on the OBHS (CMG-1T seismometer) and monitor all units for 2 min.
3. Switch on the DM24 for strainmeter component a and monitor all units for 2 min.
4. Switch on the DM24 for strainmeter component b and monitor all units for 2 min.
5. Switch on the DM24 for strainmeter component c and monitor all units for 2 min.
6. Switch on the DM24 for the PMD seismometer and tiltmeter and monitor all units for 2 min.

The CRM monitors all units. If after 1 hr the CRM has not received valid data from a unit, it will repeat the start-up sequence for that unit. This process repeats as many as 10 times if the unit continues to fail to respond. In the future, this will be modified to allow manual override.

Another process running on the CRM monitors the output from the tiltmeter and automatically nulls the output by sending the DM24 a command to drive the leveling motors if the output is >40% of full scale for more than half an hour. Each time the CRM powers up the motor drive circuitry, it makes two attempts to null the tiltmeter output. After nulling, it will not attempt to null for another 8 hr.

When the CRM receives a character to request a "command session" from the upstream SAM, it stops sending data and switches to command-session mode. In command-session mode the CRM provides features to control many other modules (i.e., master RTC, the PDM, and the strainmeter interface) in a simple command set. The available commands (those of the DM24s, SAM, and BOB, as well as of the CRM) are summarized in Table T2. The command session is finished by a "go" command from the upstream or by a time-out. When the upstream requests the CRM for a connection to a DM24, the CRM stops sending data to the upstream and relays the request of connection to the DM24. The CRM maintains the command-session link until the upstream finishes the session.

T2. Available command set for the CRM, DM24s, SAM, and BOB, p. 51.

The watchdog fail-safe timer that is a part of the H8 microprocessor reset circuit is employed to reset the CRM. The timer should be triggered at least every 1.5 s. The multitasker of the CRM system normally does this every second. If there is some failure of the CRM program, no triggering of the timer results in a reboot of the system.

Power Distribution Module

The power distribution module (PDM) is a single round circuit board that switches and distributes power to all the sensors, the DM24s, and the SAM. Supply voltage for the PDM can vary from 16.5 to 75 V. For all the DM24s, the PDM supplies power simply by switching the power on; for the SAM, it first regulates the supply to 18 V. A voltage drop in series diodes (4.4 V) plus that in the cable resistance (~24 Ω) ensures that the supply for the OBHS is below 36 V. The other DM24s operate from 36 to 75 V.

Each power channel is switched by separate solid-state relays controlled by the CRM so every component can be switched independently. The current through each power channel is monitored by the CRM every second. To protect other modules, the CRM shuts down a channel if that channel draws an unexpectedly large current for more than 30 s. The criteria to shut down, which is configured in the CRM system complementary metal oxide silicon memory, can be different for each component. The current maximum and minimum limits are set to 200 mA and 28 mA, respectively, for the OBHS and DM24s; the SAM upper limit is set to 500 mA.

Strainmeter Interface

The strainmeter interface, other than the DM24 for the strainmeter, monitors the signal and controls the valves of the strainmeter. It reports strainmeter status information to the CRM when some change occurs on these valves or upon request from the CRM. The information includes the status of all valves, signal voltages of all the channels, and the supply voltage for the interface (see "Electronic Control and Signal Conditioning," p. 8).

Downhole Link

Four 1-km-long cables, which are tied to 4½-in-diameter casing pipe, supply power for each downhole sensor as well as transfer data to the MEG. Cables for the CMG-1T seismometer and the PMD seismometer are of eight conductors each; tiltmeter and strainmeter cables are of 12 conductors each. The outside diameter of all cables is 19½ mm. The cable consists of two layers of conductors covered with an inner jacket of high-density plastic elastomer (HDPE), a tension member of aramid fibers, and an HDPE outer jacket. The fiber tension member provides tensional protection for conductors up to 1800 kilograms force (kgf) of maximum tensional load. But these cables still have enough mechanical flexibility to allow a bending radius as small as 12 in. The cables have densities of 1.12 g/cm^3 (12-conductor) and 1.05 g/cm^3 (8-conductor) so that they are almost neutrally buoyant in seawater. Thus these cables experience minimal tension in the borehole. They are also strapped to the 4½-in casing at ~7-m intervals. The cross-sectional area of conductors is, for both 12- and 8-conductor cables, 1.25 mm^2 for those in the inner layer and 0.9 mm^2 for those in the outer layer. Cable resistances for 1 km are 16 Ω for 1.25 mm^2 conductors and 20 Ω for 0.9 mm^2 conductors. Thicker conductors are chosen for the lines carrying larger currents to lower the voltage drop in the cables.

The assignment of the cable wires and the pin assignment of connector pins on both the MEG UMC and the sensors are summarized in Table T3.

T3. Pin assignments of Ocean Design UMCs, p. 52.

SAM

The SAM is the recorder mounted in the top of the battery frame. The SAM is connected through an oil-filled cable to the MEG. When the storage capacity of the SAM becomes full after ~1 yr of recording, an ROV can replace it with an "empty" SAM. Ejection of the SAM is aided by a lever mechanism on the frame (see Fig. F16).

F16. Photograph of SAM unit for recording up to 72 GB of data, p. 38.

The SAM receives data from the MEG through a high-speed (57,600 bps) RS232C serial link, which buffers the data in a silicon file that consists of 64 MB of flash memory of which 56 MB are allocated for buffering. The flash file is nonvolatile memory so that data in memory will not be lost even during loss of power. The amount of data incoming to the SAM is expected to be 12 kbps in a standard configuration of recording (i.e., three channels of the CMG-1T seismometer at 100 sps, three channels of the PMD seismometer at 20 sps, nine channels of the strainmeter at 50 sps, and two channels of the tiltmeter at 4 sps). In this configuration, the buffer memory will be filled in about half a day.

As the buffer becomes full, the SAM flushes the contents of the memory to a hard disk drive (HDD). The SAM has four HDDs of 18 GB each, for a total of 72 GB of storage. The HDDs are powered only on the memory flush, and only one disk drive is activated to spin up, whereas the other HDDs are kept in standby mode. It takes ~1 min to transfer 1 MB of data onto a disk.

The HDDs are powered by NiMH batteries in SAM, while the other components run directly on power from the MEG. The voltage of the NiMH battery pack is 14.0 at full charge. Use of the NiMH batteries prevents the transient large surge current of the HDDs from affecting the rest of the system. These batteries are recharged after the HDDs have consumed approximately half the capacity of the batteries on each buffer flush. After the batteries are fully charged, the charging mode is switched to trickle charge. Power consumption of the SAM is ~1.6 W in noncharging mode. When the batteries are being charged, the power consumption is higher. The limit of the charging current, typically 150 mA, can be specified by a user.

The directory of the data written on the disk can be browsed by "dir" command on the infrared (IR) port, though the data cannot be replayed through the serial link. On the dir command, the SAM will reply with a list of system ID, stream ID, the date of the first data, the date of the last data, and the total amount of data for a stream. The disk drives can be connected to personal computers (PCs) with a SCSI interface. A PC program called "Scream!" can replay the data written on the disk in GCF.

In parallel to saving the received data into the buffer memory, the SAM also sends the data, together with SAM status information, to the IR port on its top, which is the link for the BOB module. The IR serial link also allows the SAM to receive a command-session request from the upstream BOB module; if the request is addressed to the CRM or downstream modules the SAM relays them to the CRM.

BOB

The BOB module is a temporary recording device for short-term use (Fig. F17). An important purpose of the BOB module is to make an initial diagnosis of the system status by ROV either by watching light-emitting diodes (LEDs) on top of the BOB module or by communicating to the system through an ROV cable connected to the BOB module.

F17. Photograph of the BOB communication link between ROV and NEREID, p. 39.

A Subconn eight-pin underwater connector is attached to the side of the BOB module. The connector functions both as a serial link to an ROV and as a power switch for the BOB module. The serial link allows communication from a surface ship to the whole system via a cable to the ROV. The speed of the ROV serial link can be configured over a wide range (75 bps–112 kbps) so that it can match the capability of an ROV. The BOB module is run by two internal 18-ampere-hr (Ah) lithium batteries, and the batteries are switched by connecting either the ROV cable or a switch plug to the connector.

An ROV may place the BOB module on top of the SAM so that the IR ports on the SAM and BOB module are aligned for communication. The BOB module receives data sent by the SAM through IR port and stores it in its flash memory. The capacity of the flash memory is 256 MB, which corresponds to storage of about a 2-day record for a standard sensor setting.

The LED matrix display on top of the BOB module shows the status of the MEG, SAM, and sensors. Each pixel of the LED matrix display corresponds to a particular set of system ID and stream ID. The LED has two colors: green indicates a reception of the data block and red indicates a reception of the status block. The assignment of the position of the LED and the stream ID (cf. Table T1) is shown in Table T4. The LEDs are visible through a 50-mm-diameter sapphire glass window on top of the BOB module.

T4. LED chart for BOB's system diagnostics matrix display, p. 53.

The power consumption of the BOB module is ~1 W, and the data written in the flash file are readable through the ROV serial link.

Power Consumption of the System

The whole system is operated with limited SWB power. Although a short-term power increase can be supplied by an accumulator in the battery system, the system will fail eventually if the long-term average power consumption is more than the capacity of the battery system. Thus, the power consumption of the system was carefully evaluated before the deployments for the systems in both Sites 1150 and 1151.

Figure F18 shows the result of the power consumption measurement for the NEREID system in Hole 1151B. The power consumption is 18.1 W when the SAM charges the NiMH batteries for the HDD and 15.8 W otherwise. These values are a little greater than the expected values at the seafloor because they were measured while the sensors were experiencing large ship-driven motions.

F18. Result of the system power consumption measurement for Hole 1151B system, p. 40.

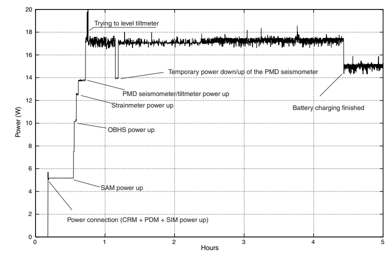

In the NEREID system for Hole 1150D, the three-component strainmeter was installed. The system for Hole 1150D consumes ~2 W more power than does the system for Hole 1151B in which a single-component strainmeter was deployed. The difference in the power consumption comes mainly from (1) the two additional DM24s for the Hole 1150D system that digitizes six extra channels and (2) the additional sensors in the strainmeter. The increase of the data obtained also shortens the disk-writing interval, which results in an increase in the duty cycle of the NiMH battery charging.

The SWB power supply is rated at 18 W, but the actual power depends on environment factors (see **"Seawater Battery,"** p. 17). For either system power consumption is almost at the limit of the capacity of the SWB system. Plans are in hand to modify the electronics to decrease power consumption.

POWER SUPPLY

Seawater Battery

The power for all the NEREID system is supplied by the SWB system, which consists of three SWB1200 (Kongsberg Simrad, Norway) cells (Hasvold et al., 1997), a DC/DC converter, and an accumulator. The cell is a magnesium/oxygen battery based on a magnesium anode (negative electrode) that uses seawater as the electrolyte and oxygen dissolved in the seawater as the oxidant.

The chemistry of the cell is the dissolution of magnesium at the anode, given as

$$2Mg = 2Mg^{+} + 4e^{-}, \qquad (1)$$

and consumption of oxygen at the cathode,

$$O_2 + 2H_2O + 4e^{-} = 4OH^{-}, \qquad (2)$$

which is written in a simplified form

$$2Mg + O_2 + 2H_2O = 2Mg(OH)_2. \qquad (3)$$

The formation of an alkaline at the cathode surface may lead to the formation of a calcareous deposit as follows:

$$4Ca_2^+ + 4HCO_3^- + 4OH^- = 4CaCO_3 + 4H_2O. \quad (4)$$

The alkaline reaction products need to be removed from the cathode surface by sea current because the calcareous formation disturbs the reaction (Equation 2) at the cathode.

The anodes are AZ61 magnesium alloy rods with a diameter of 184 mm and a length of 2200 mm, including the anode connector device. The anode can be replaced by ROV and is surrounded by the cathodes suspended from the titanium frame (Fig. F19). The weight (in air) of each anode is 110 kg and that of the titanium cathode frame is 62 kg. The cathode element consists of a titanium wire core with carbon fibers oriented radially (Fig. F20). The carbon fibers allow rapid material transport and high current density. The cathode collector lead is connected to the titanium frame, which is also part of the cathode. The titanium frame allows seawater to pass easily through the cells so that oxygen-rich seawater is supplied to the cathode and the products of the cell reactions are removed.

The obtainable cell voltage is ~1.6 V, although this depends largely on the conductivity of the seawater, which may vary with temperature and salinity. The catalytic effect of bacteria colonizing on the cathode surface, which was observed on all seawater cells in previous deployments of the system, is another of the many factors affecting the cell voltage. The maximum cell power is limited by the rate of the supply of oxygen to the cathode. The oxygen supply rate is proportional to the oxygen concentration in the seawater and the speed of circulation. To produce the designed output of 6 W for each cell, a minimum circulation of 20 mm/s, oxygen concentration of 3 ppm, and minimum salinity of 20‰ is required. At Sites 1150 and 1151, where the water depth is ~2500 m, an oxygen concentration of ~2.7–3.6 ppm is expected based on previous study near these sites (M. Kawabe, pers. comm., 1998).

Because the cells have an open structure, the isolation between them is low, which leads to large leakage currents in serially connected cells. The cells are consequently connected in parallel. The DC/DC converter changes the low cell voltage (1.6 V) into the output voltage (42.0 V). The output of the DC/DC converter is fed to the accumulator that averages the power demand on the DC/DC converter and the seawater cells. After deployment of the cells, the DC/DC converter is inactive until the cell voltage becomes >1.54 V. After the cells are activated, the DC/DC converter takes power from the cells and charges the accumulator as long as a sufficient cell voltage (>1.28 V) is available. If the cell voltage becomes lower than that threshold, the DC/DC becomes inactive until the cell voltage is restored to 1.54 V. The low threshold depends on the status of the accumulator cell charge. The lower the cell charge is, the lower the threshold becomes. The lowest threshold is ~1.28 V. The accumulator consists of multiple 2-V Cyclon (Hawker Energy) lead acid cells that form a 5-Ah 36-V cell in total. The accumulator cell is float charged by the DC/DC output. The voltage of the accumulator output is 42.0 V when the accumulator cell is fully charged and has no charging voltage applied by the DC/DC converter. The cell is stored in a 6500-m depth-rated pressure housing that has four-pin GISMA series-10 underwater connectors for the load output and the DC/DC converter. The DC/DC converter is also stored in a similar pressure housing but has two Subconn one-way underwater power connectors for the SWB cells and the GISMA connector for the accumulator.

F19. SWB1200 cell structure, p. 41.

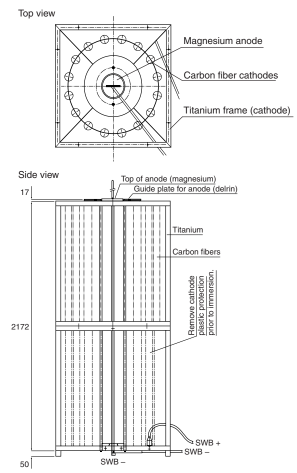

F20. Structure of the carbon fiber brush used in the cell cathode, p. 42.

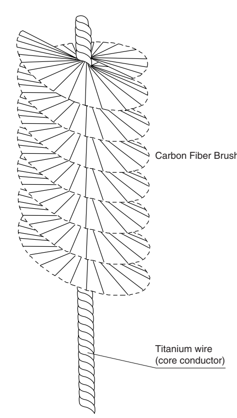

Battery Frame

The SWB system is mounted on the PAT, as shown in Figures F21 and F22. The three SWB cells are stored in concentric positions. The PAT is made of ordinary angle steel that is zinc coated; the base is coated with tar epoxy paint to protect it from corrosion. The titanium frame of the SWB cell and the stainless-steel pressure housings for the DC/DC converter and the accumulator are mounted on the PAT with polyvinyl chloride insulators. The top of the PAT is a white, flat panel made of fiber-reinforced plastic (FRP) drainboard that has access holes for the SWB anodes. The flat panel, which viewed from above is circular, serves as the ROV platform and is supported by a metal frame. The diameter of the top plate is 3200 mm. The bottom structure of the PAT is also circular, and the diameter is 3658 mm, which corresponds to the diameter of the reentry cone. The bottom leg is 240 mm in height. The battery cells are elevated above the reentry cone to improve seawater circulation through the cells. The center bottom part of the PAT contains coaxial rings placed to guide it smoothly over the riser assembly on its installation. The hole in the top center part of the PAT provides space for the MEG frame. The total height of the PAT is 2640 mm to accommodate the SWB cells. The vertical position of MEG on the riser is set to allow ROV service.

The PAT also holds the SAM recorder frame beneath the PAT top panel. The top part of the SAM recorder protrudes from the panel. The SAM recorder can be lowered into the hole of the frame panel so that the UMC at the bottom of the SAM bulkhead is mated by gravity force to a UMC receptacle on the stab-plate placed in the SAM frame. In the lowering operation the hole keeps the SAM canister upright; a key on the bottom bulkhead of the SAM canister aligns with the keyway in the hole to provide correct orientation for mating the UMC. The cable from the UMC receptacle has a T-junction: one branch is connected to the SWB system and the other goes to a receptacle mounted on the FRP panel. An installed cable on the panel is used by the ROV to connect the UMC receptacle to the MEG canister. Initially, the ROV cable is fastened to the top panel by fastening mechanisms and a parking connector for the ROV plug. In September 1999, the ROV removed the fasteners and connected the ROV's UMC plug to the MEG canister. The SAM recorder can be ejected with help from an ROV-operated lever mechanism in the SAM frame (Fig. F23). The lever can be locked at two positions: one at the mated position of the SAM and the other at the released position. By using the locking positions, the ROV can easily replace the SAM recorders.

F21. Side-view drawing of the power access terminal (PAT) on top of the reentry cone, p. 43.

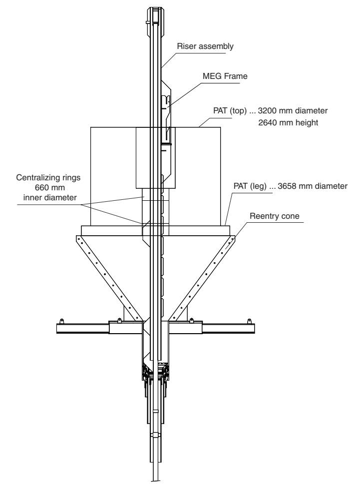

F22. Photograph of the PAT from above the moonpool, p. 44.

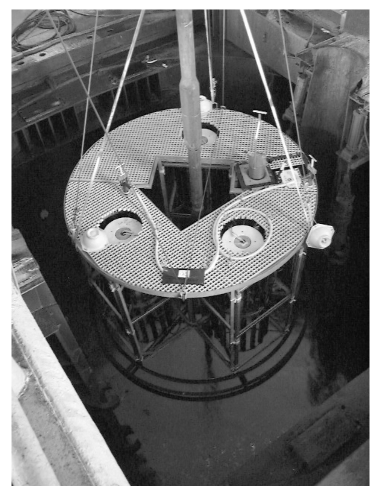

F23. Photograph of the recorder frame with the SAM in place, p. 45.

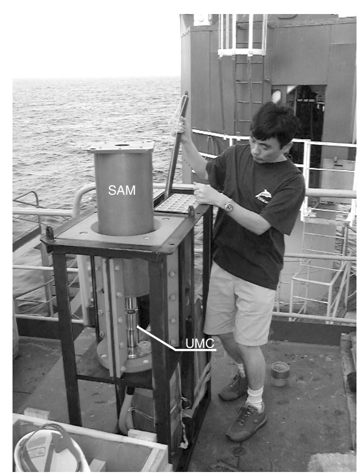

OPERATION

Operation of NEREID Observatories

As soon as the NEREID systems were installed during Leg 186, the SWBs started charging the accumulators (see "Power Supply," p. 17). The downhole sensor strings, however, do not start functioning until an ROV arrives at the site to start the system (i.e., to connect the modules in the PAT electrically to the MEG). In the present NEREID design, the MEG and the downhole sensor string are physically connected by 4½-in casing pipe so that they are installed with electrical connections made up, whereas the PAT is not electrically connected. This is because the PAT cannot be lowered with the 4½-in casing pipe assembly because the reentry of the sensor string into the cone requires the use of the vibration-isolated television (VIT) camera and visibility to the stinger. The PAT would block the view, making reentry impossible. Furthermore, both the VIT camera and PAT must be suspended by cables, which could become tangled if deployed simultaneously.

The NEREID system operation first requires an electrical connection to be made between the PAT/SAM and the MEG. This was the mission of the *Dolphin 3K* of the Japan Marine Science and Technology Center in early September 1999 (see **"Borehole Instruments,"** p. 58, in the "Site 1150" chapter) (Fig. **F24**). Once this connection is made, the data from downhole start to flow into the SAM on the PAT, which can store 72 GB, enough for ~1 yr of data from all the sensors (see **"Borehole Instruments,"** p. 5). The ROV can check the status of the system via a BOB module, which seats on the SAM and communicates through a sapphire window using IR communication. If there is no problem, the ROV needs only to replace the SAM at least once every year to prevent loss of data continuity.

A seafloor downhole observatory is still at pilot-study stage. There is no set routine on which to rely. In our design the sensor string is unrecoverable for the reasons given in **"Installation Techniques,"** p. 3. Therefore, the string must be composed of reliable instruments (see **"Borehole Instruments,"** p. 5). On the other hand, the seafloor components are replaceable and serviceable by a submersible vehicle. The BOB module may be considered a communication extension of the ROV. The SAM is replaced at each ROV visit. The MEG can be pulled out of its seating frame and reinserted by the ROV, although the operation is more complex than other tasks.

The battery life is somewhat unpredictable because it depends on the bottom-water current, dissolved oxygen, and the actual power consumption of the system over a long period of time. Since the battery operates only in the water, separate tests were conducted for the battery and for the rest of the system. We expect a 2- to 3-yr life span, within which time period we will have collected and analyzed the data quality and obtained preliminary scientific results.

F24. Photograph of the JAMSTEC ROV, *Dolphin 3K*, p. 46.

Future Cable Connection

In June 1996 an underwater cable system was constructed off Sanriku (northeast Japan) by the University of Tokyo Earthquake Research Institute to continuously monitor earthquakes and tsunamis. The cable was deployed to be perpendicular to the trend of the Japan Trench and is landed at Kamaishi, Iwate Prefecture, at ~39°15′N. The cable system covers the area where water depth is <2500 m. The eastern end of the cable is near Site 1150.

Three seismometers and two tsunami gauges are connected to the cable system. The seismometers are servo-type accelerometers and the tsunami gauge is a crystal oscillator type. Data from the sensors are digitally transmitted using optic fibers in the underwater cable to the land station at Kamaishi. From there the data are distributed to universities and governmental institutions in Japan through Tohoku University.

The multioptic-fiber type of cable system is extendable with six unused cables. Currently there is a plan to connect an extended 200-km-long cable at the end of the present cable and to add six seismometers and two tsunami gauges to the cable system. The planned cable runs east and south from the end of the present cable. We plan to connect NEREID-1 at Site 1150 and NEREID-2 at Site 1151 using these spare optic fibers, thus supplying power to the NEREID observatories and enabling real-time transmission of signals from the NEREID sensors to land.

The deployed seafloor seismometers and tsunami gauges in pressure vessels are directly connected to the optic cable, but the NEREID system requires a branch cable from the main optic cable. Because a long branch cable causes loss of electronic power, a branch cable should be no longer than a few kilometers. The suggested cable route to connect the NEREID systems is shown in Figure F25. By deployment of a branching unit (BU) near the NEREID system, a maximum of 30 W can be supplied from the cable system. The present NEREID system requires ~18 W, so we may add more sensors on the seafloor to the present system.

The MEG of the NEREID system has a UMC to communicate with the NEREID system and to supply power. In the present system, the MEG is connected to the PAT which has SWBs and to the SAM through the ROV cable. We can supply power to the whole system and can control the system through the UMC on the MEG. Data from all sensors can also be retrieved through the UMC. Therefore, we can connect the underwater cable to the UMC on the MEG in place of the PAT. We do not need any changes of the MEG or the sensors to connect to the cable system. We do need, however, an optical/electric conversion unit (OEC) (Fig. F26) to connect the NEREID system to the cable system because the control of the system and retrieval of data are performed using an RS-232C line. An ROV can connect a bidirectional OEC and the MEG using an ROV cable with the UMC.

Of the 12 optic fibers in the cable, six are already used for deployed seismometers and tsunami gauges and four are reserved for future cable extension (Fig. F27). Two fibers are available for real time data transmission from the NEREID systems. The BU includes a branching circuit that divides the optic fiber. In addition, each circuit has a function to select signals for itself and transmit the signals to the NEREID system. For data transmission from the NEREID system, the branching circuit makes a multiplexed data transmission. An optic fiber with a large bandwidth can handle the multiplexed data transmissions of two NEREID systems.

Connection of the NEREID system to the cable system has many advantages: (1) data are distributed in real-time, (2) system settings can be changed at any time, (3) power is supplied continuously, and (4) there is no limitation of observation time. After confirmation of data quality from the present NEREID system, we will begin designing each unit of the cable system for connection between the NEREID system and the cable system. The data from the NEREID systems will be distributed via the Internet.

F25. Layout of the existing fiber-optic cable system of the University of Tokyo, p. 47.

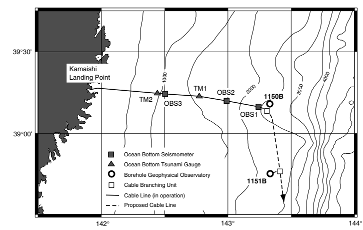

F26. Connection schematics of NEREID systems to the existing fiber-optic cable by use of BUs, p. 48.

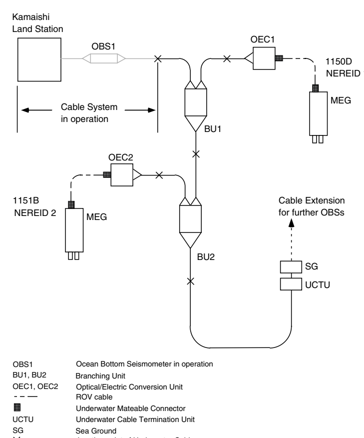

F27. Fiber-optic cable system diagram, p. 49.

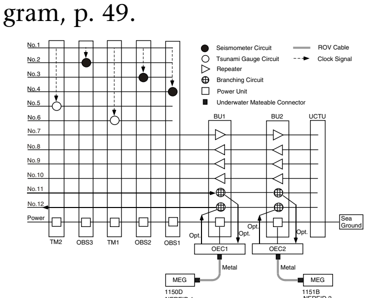

REFERENCES

Hasvold, Ø., Henriksen, H., Melvær E., Citi, G., Johensen, B.Ø., Kjønigsen, T., and Galetti, R., 1997. Sea-water battery for subsea control systems. *J. Power Sources,* 65:253–261.

Linde, A.T., Agustsson, K., Sacks, I.S., and Stefansson, R., 1993. Mechanism of the 1991 eruption of Hekla from continuous borehole strain monitoring. *Nature,* 365:737–740.

Linde, A.T., Gladwin, M.T., Johnston, M.J.S., Gwyther, R.L. and Bilham, R.G., 1996. A slow earthquake sequence on the San Andreas fault. *Nature,* 383:65–68.

Linde, A.T., Sacks, I.S., Johnston, M.J.S., Hill, D.P., and Bilham, R.G., 1994. Increased pressure from rising bubbles as a mechanism for remotely triggered seismicity. *Nature,* 371:408–410.

Linde, A.T., Suyehiro, K., Miura, S., Sacks, I.S., and Takagi, A., 1988. Episodic aseismic earthquake precursors. *Nature,* 334:513–515.

Ocean Drilling Program, 1996. *Understanding Our Dynamic Earth through Ocean Drilling: Ocean Drilling Program Long Range Plan Into the 21st Century:* Washington (Joint Oceanographic Institutions).

Sacks, I.S., Linde, A.T., Snoke, J.A., and Suyehiro, S., 1981. A slow earthquake sequence following the Izu-Oshima earthquake of 1978. *In* Simpson, D.W., and Richards, P.G. (Eds), *Earthquake Prediction: An International Review.* Am. Geol. Soc., Maurice Ewing Ser., 4:617–628.

Sacks, I.S., Suyehiro, S., Evertson, D.W., and Yamagishi, Y., 1971. Sacks-Evertson strainmeter: its installation in Japan and some preliminary results concerning strainsteps. *Pap. Meteorol. Geophys.,* 22:195–208.

Figure F1. Schematic view of the NEREID borehole geophysical observatory. Detailed descriptions of each component are given in **"Installation Techniques,"** p. 3. ROV = remotely operated vehicle; PAT = power supply access terminal; DTM = Department of Terrestrial Magnetism (Carnegie Institution of Washington) strainmeter; AGI = Applied Geomechanics, Inc., tiltmeter; CMG and PMD = seismometers.

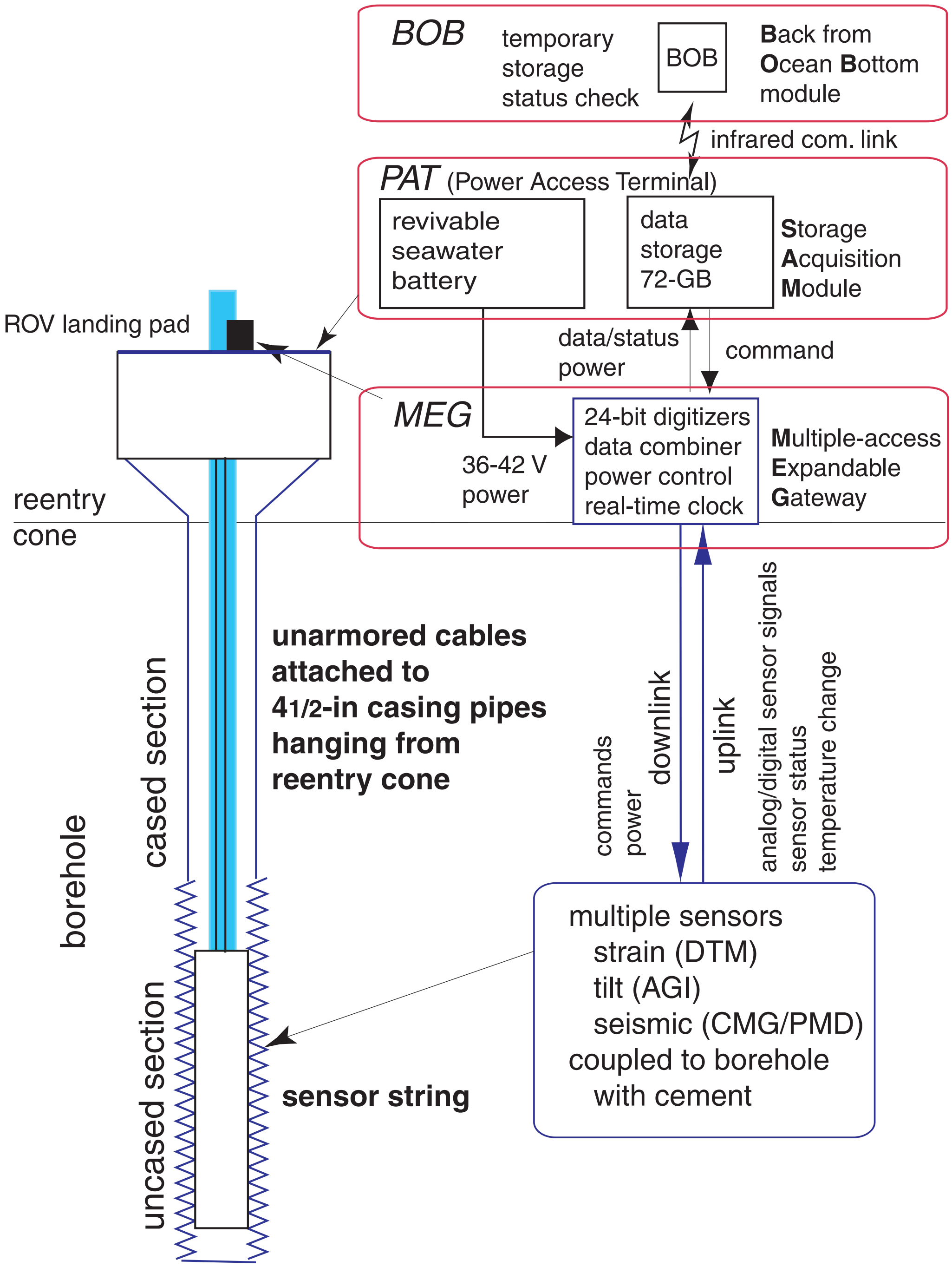

Figure F2. Instrument installation technique. The instrument string hangs on 4½-in casing pipe, which in turn hangs on the riser support just below the reentry cone. Cables from the sensors are strapped to the casing pipe and protected by centralizers. Cement is pumped through the casing pipe, through the strainmeter, and out the bottom of the stinger. Sufficient cement is pumped to fill the bare hole and to extend into the 10¾-in casing. The sensors are thus intimately connected to the bare rock. A circulating dart follows the cement/water column down the drill pipe; this dart opens a port in the casing pipe ~400 m above the instruments. This enables flushing of the drill pipe without uncoupling from the seafloor assembly, which is required to guide the battery frame into position later.

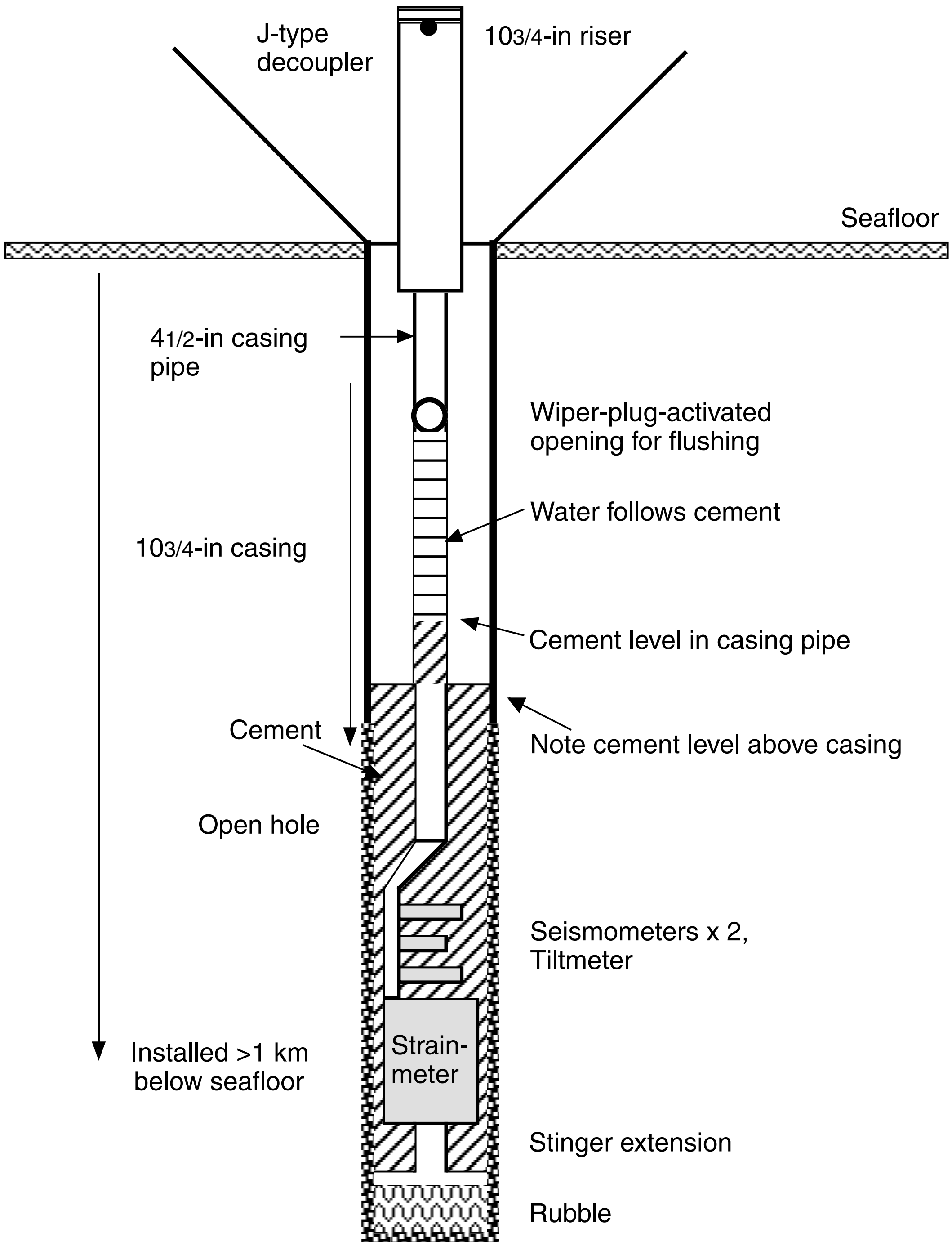

Figure F3. Schematic of the instrument environment at Hole 1151B. Note that the coupling tube supporting the seismometers and the tiltmeter is offset, allowing the casing pipe and strainmeter to be centered in the hole.

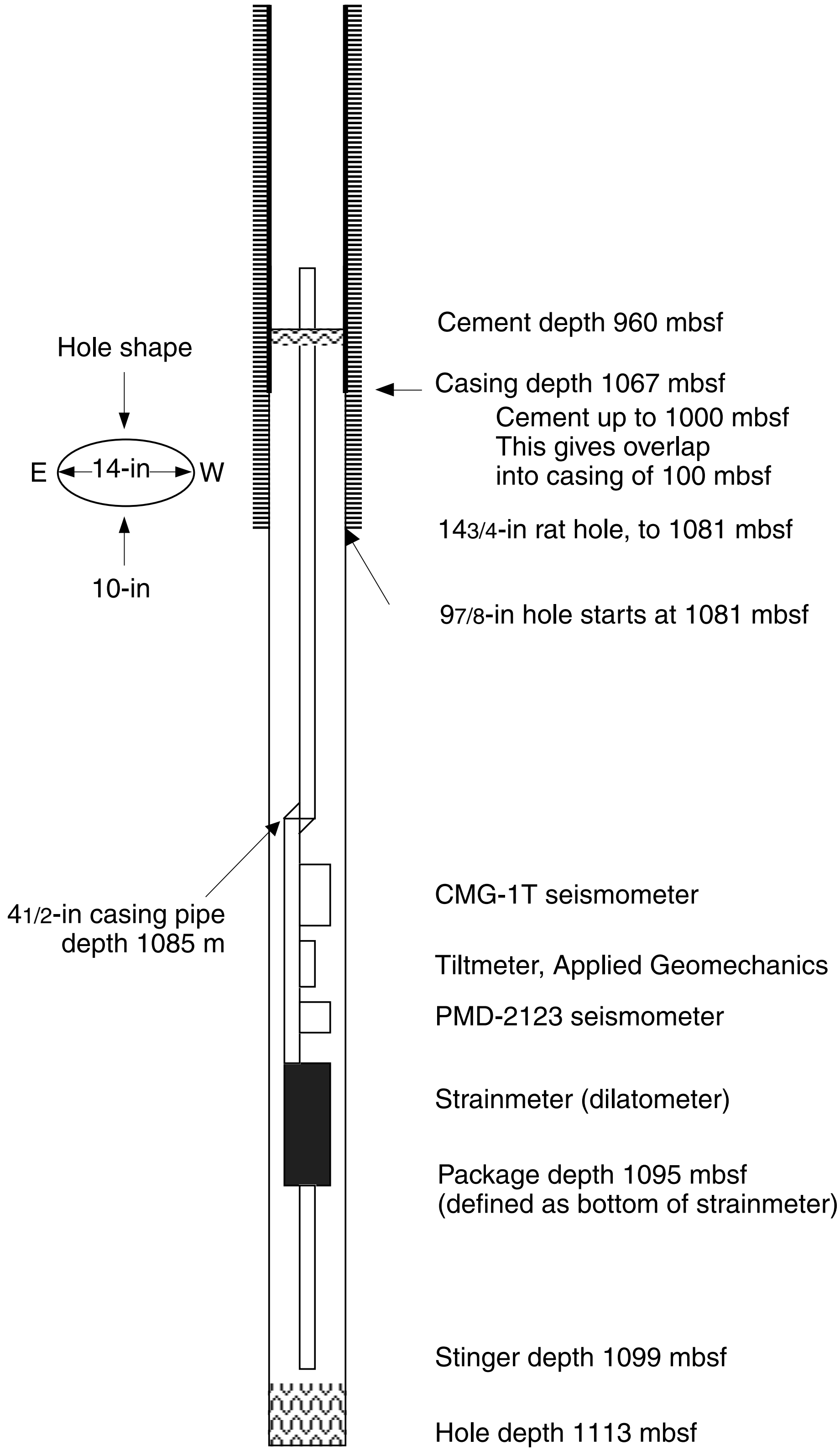

Figure F4. Schematic representation of the basic principles for the Sacks-Evertson strainmeter. The strainmeter is connected to the rock by grout so that the resilient body of the instrument is compressed and can then accurately follow subsequent changes in deformation of the surrounding rock. In normal operation the valve (V) is closed. As the sensing volume changes due to earth deformation, the top of the bellows (B) moves up or down. Since the ratio of sensing volume to bellows area is very large, the instrument employs high hydraulic amplification, which gives it extreme sensitivity. The core of a differential transformer (DT) is connected to the top of the bellows with the body (coils) of the DT fixed relative to the top of the sensing volume. A valve can be opened and closed by the control electronics so that the sensing system is maintained near the neutral position. When the valve is opened, oil can flow between the sensing volume and the reservoir (R). An expansion space above the reservoir is provided so that the overall pressure in the oil does not change significantly as the instrument is deformed.

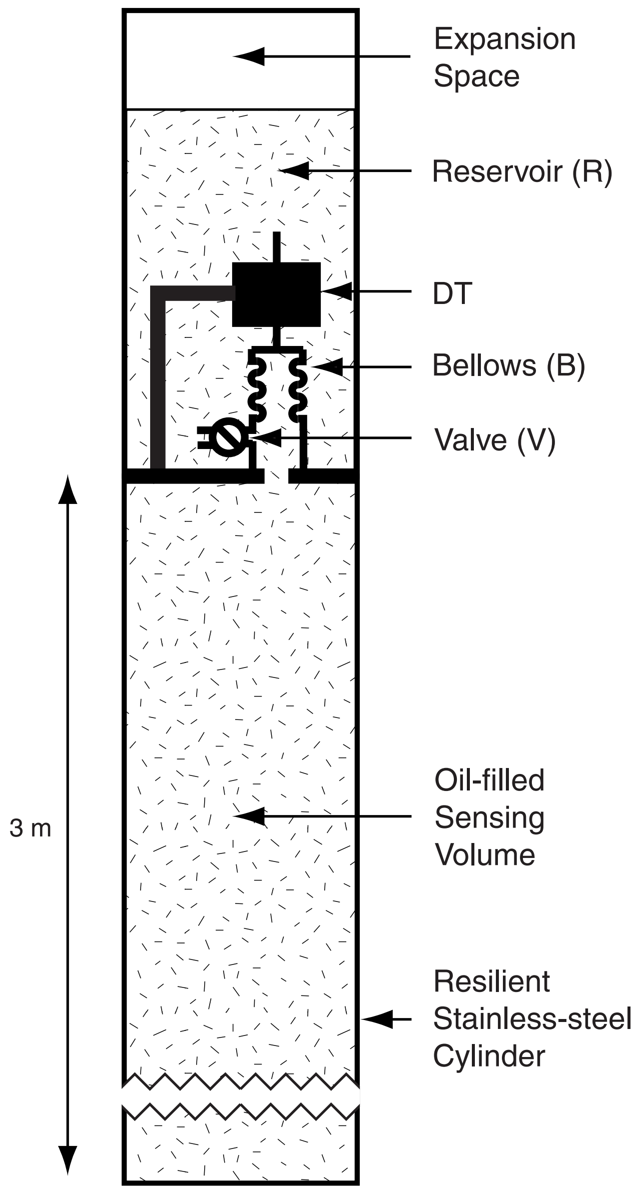

Figure F5. Schematic diagram for the dilatometer deployed in this experiment. The principle is the same as for the original design (Fig. **F4,** p. 26) but significant modifications are required. The walls are thick enough to withstand the high pressure at the installation depth. An open tube allows cement to be pumped through the instrument. The sensing volume is nearly filled with solid aluminum to decrease the volume of oil (see cross section). This lowers the thermal sensitivity of the sensor and decreases loss of sensitivity due to the oil's compressibility. We also incorporate a second bellows-differential transformer-valve assembly to ensure no data loss when the valves are opened to equilibrate the instrument; only one valve can be open at a time. DT = differential transformer.

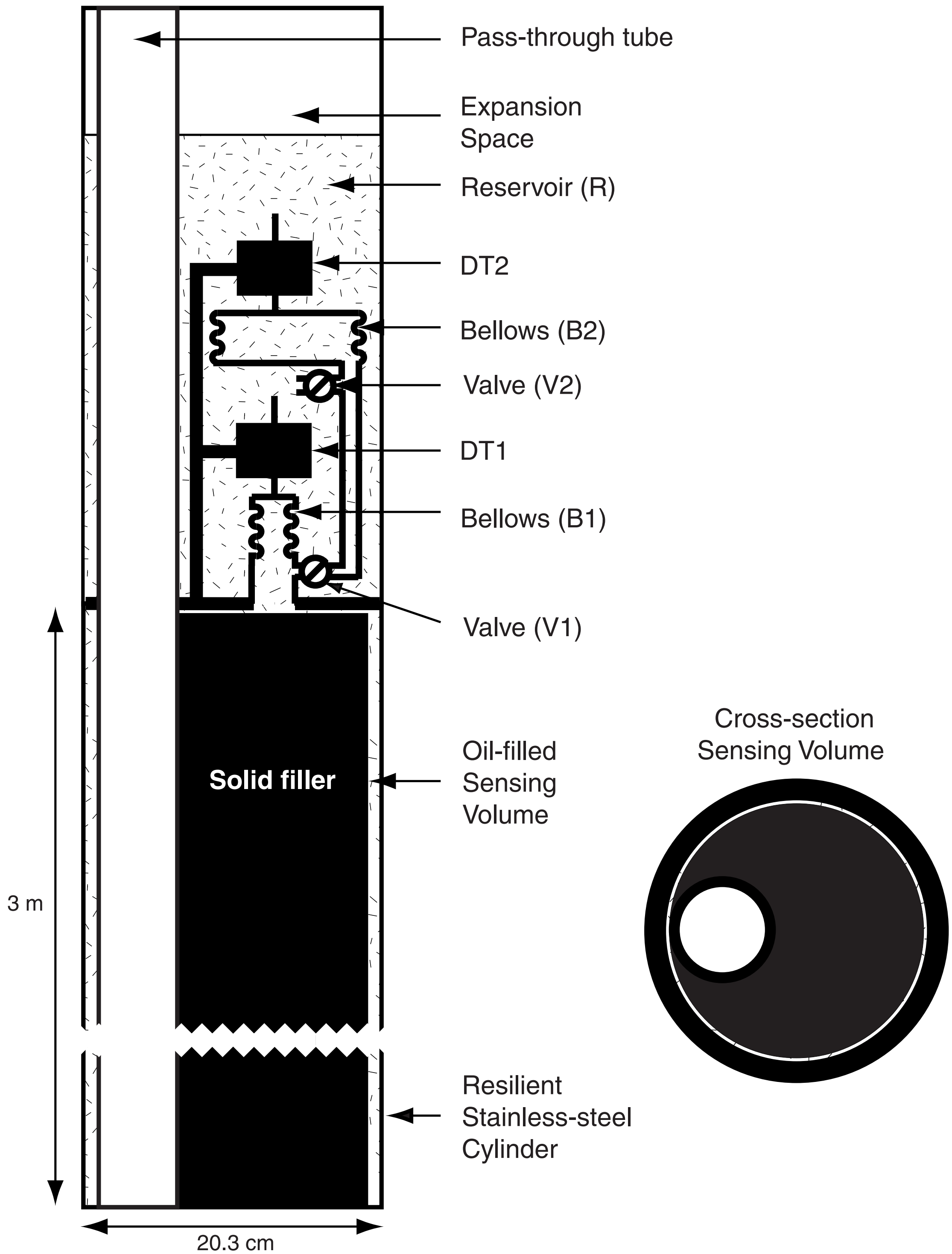

Figure F6. Block diagram of the strainmeter control electronics. The dashed vertical line separates downhole components from those on the seafloor. Regulated voltage from the SWB powers the differential transformers (DTs) (different supplies are needed for the two types of strainmeter). Output signals from the DTs are fed to both a 16-bit analog-to-digital (A/D) converter for instrument control and to 24-bit A/D converters for data acquisition. An RS232 serial link is provided so that commands can be issued remotely (via CRM; see Fig. **F13,** p. 35) to operate the strainmeters.

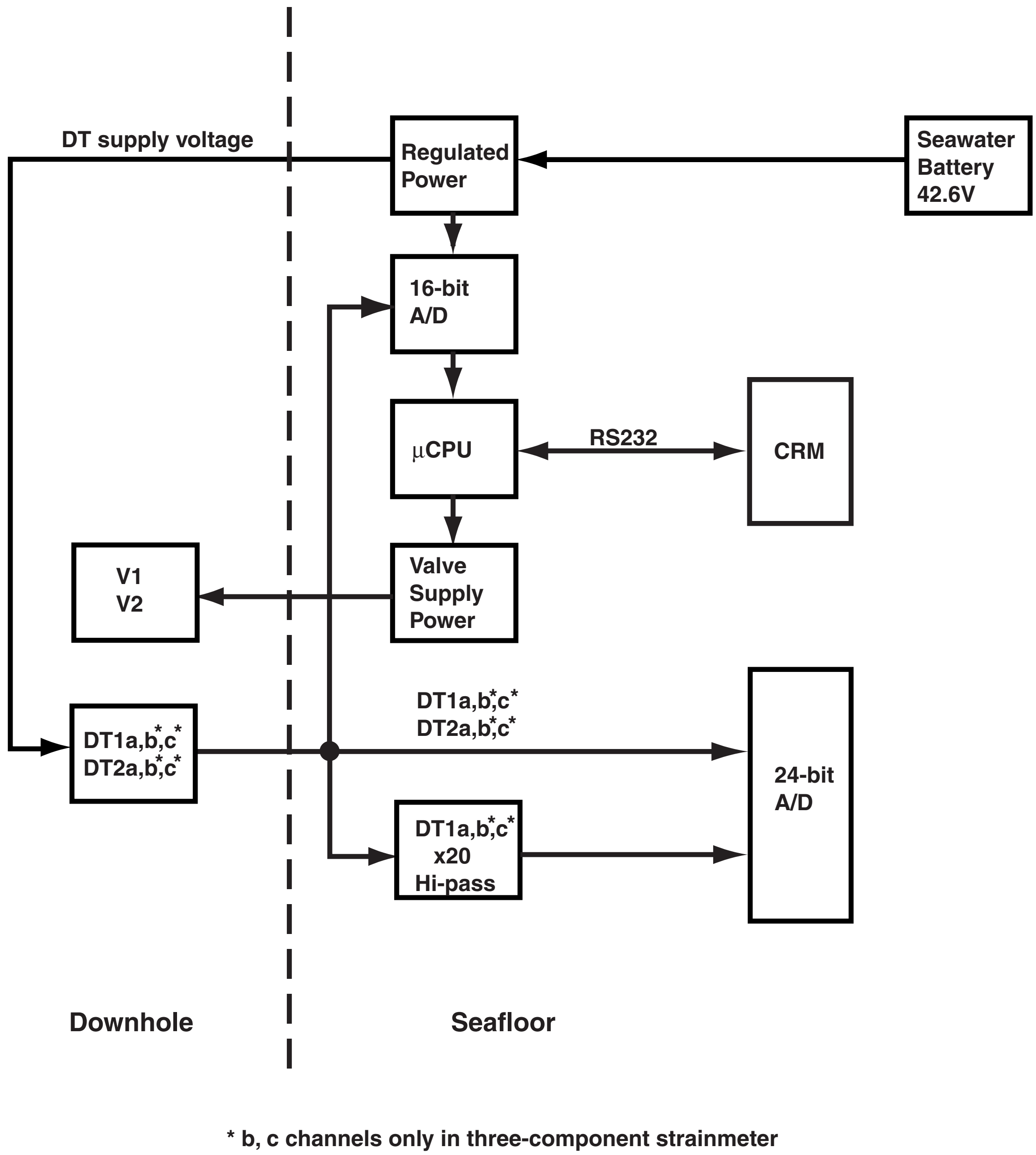

Figure F7. Schematic diagram for the three-component strainmeter. This is similar to the dilatometer (Fig. F6, p. 28), but the sensing volume is divided into three sections (see cross section), each with two sets of the bellows-differential transformer-valve sensing subsystem. DT = differential transformer.

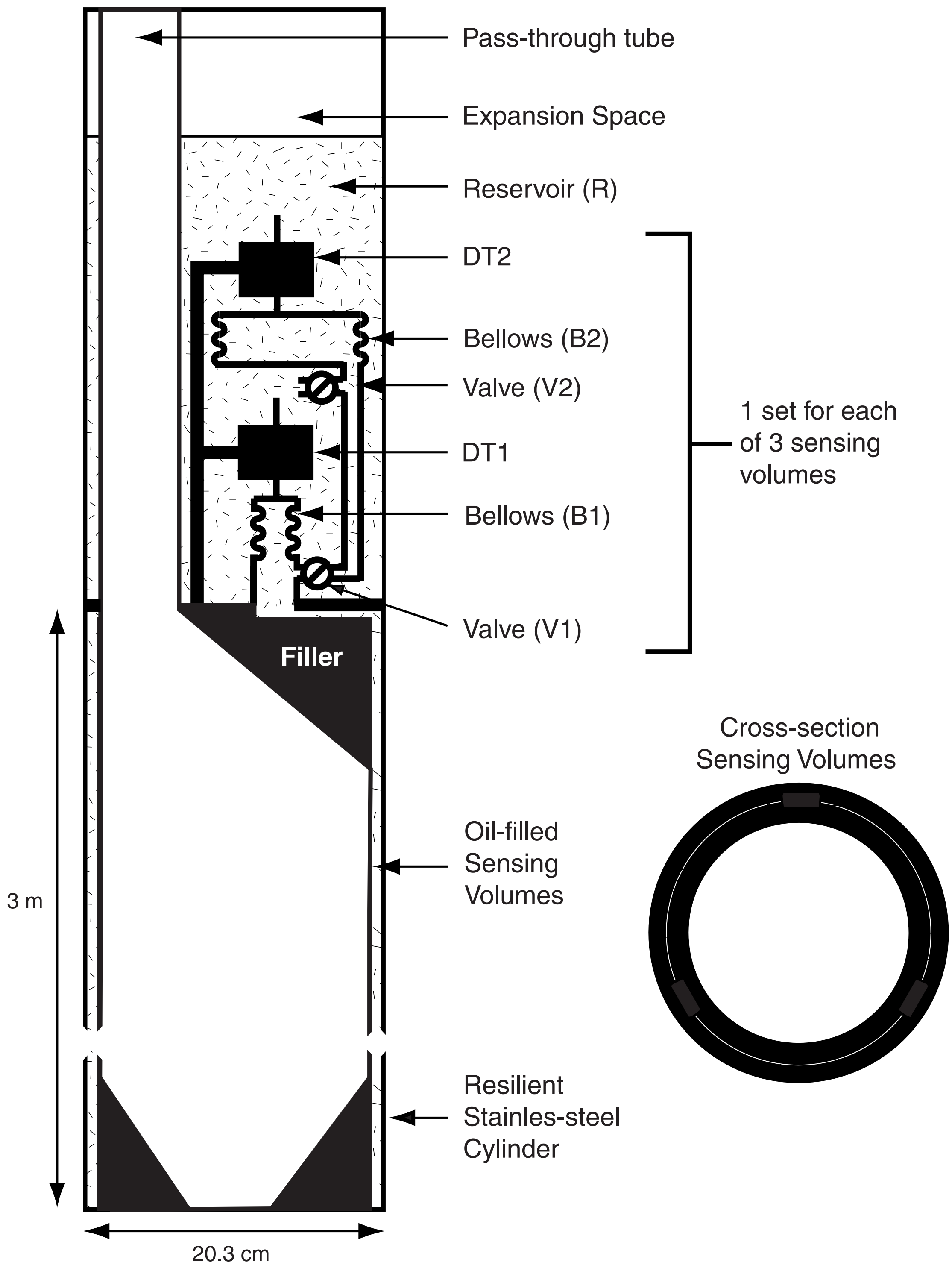

Figure F8. Outline drawing showing the OBHS components in the canister.* The undersea connector on the top bulkhead is an 8-way Subcon stainless-steel base connector. The DM24 and the sensor stack are connected by a cable to the miniature 26-way D-type connector on top of the sensor stack.

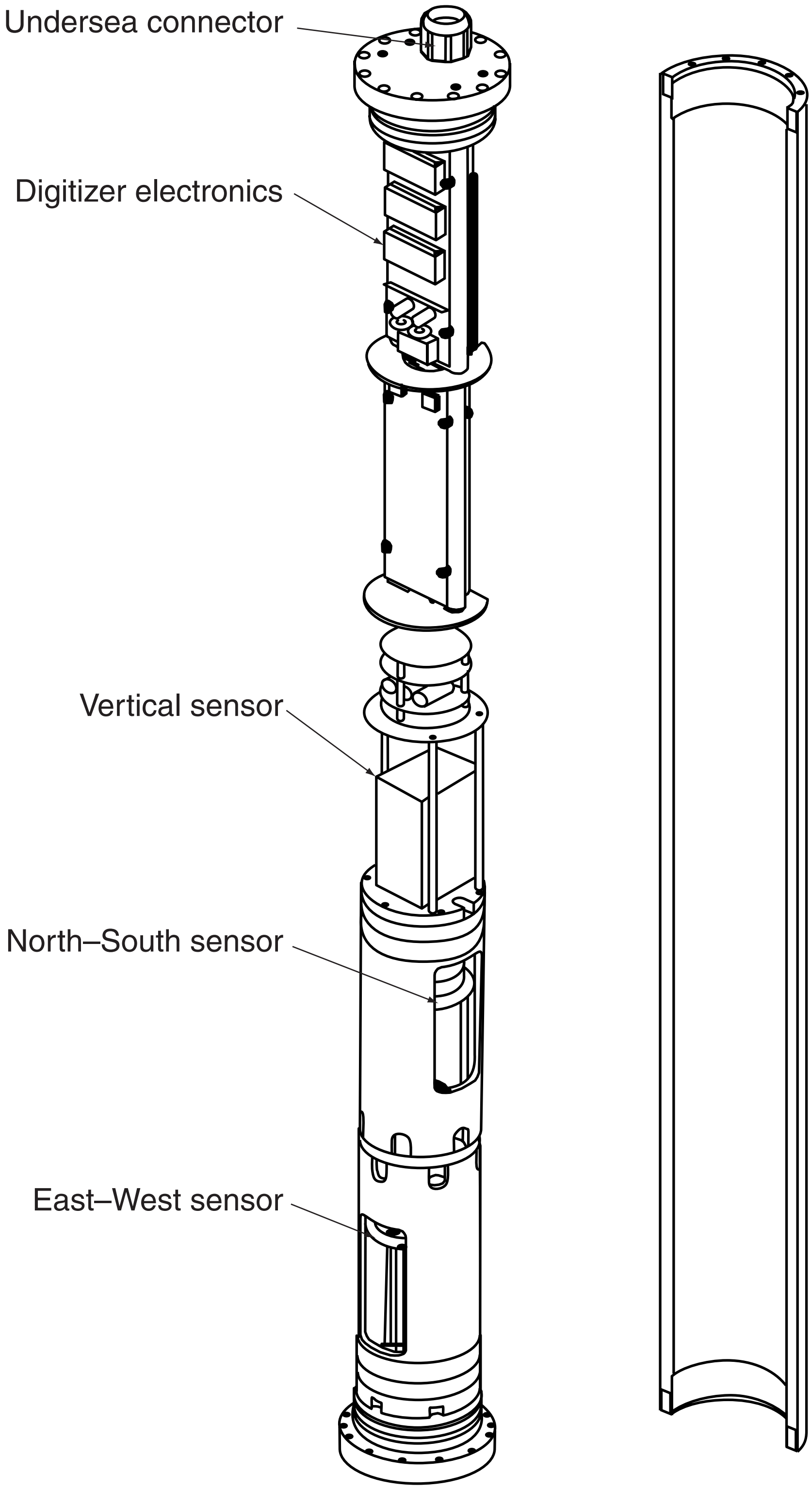

*Reproduced with permission of Guralp Systems Ltd.

Figure F9. Schematic diagram for the electronics circuits of the CMG-1T sensors. The seismometer power and the SOH circuitry are common for all three sensors, whereas the other parts are in separate units for each sensor.

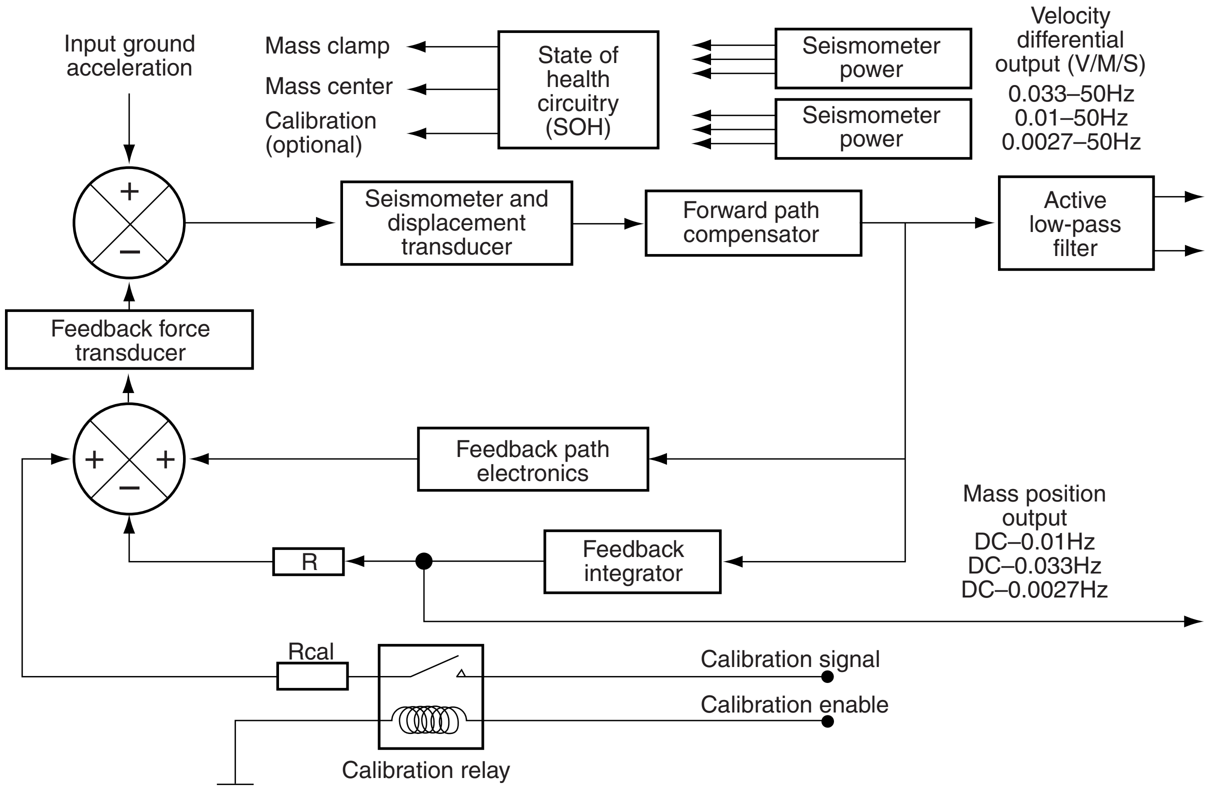

Figure F10. Comparison of noise power spectral density of the PMD-2123 and CMG-1T seismometers installed in a borehole at Nokogiriyama. The PMD has higher long-period noise.

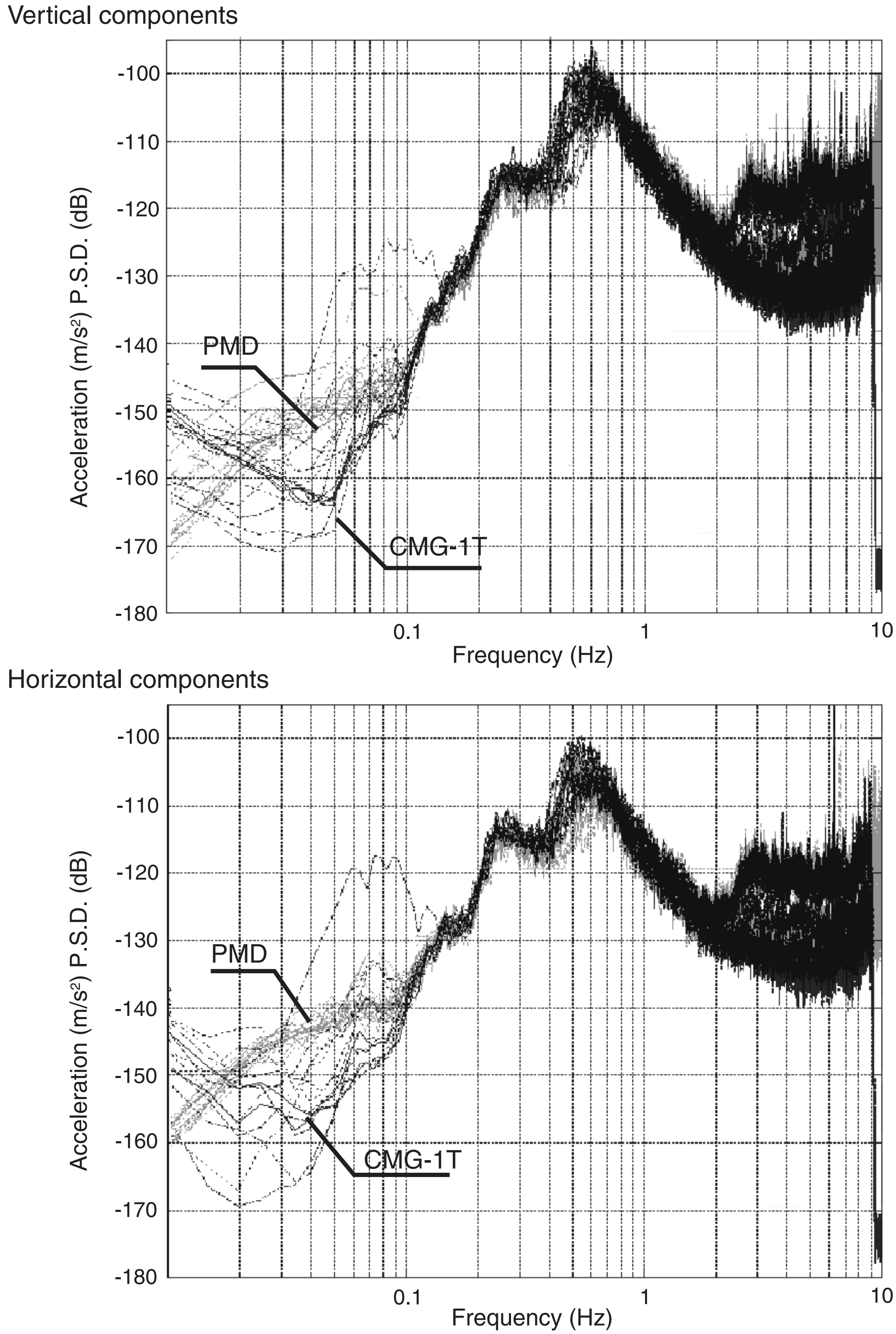

Figure F11. A schematic representation of the principle of operation of the tilt sensors. **A.** The physical sensor that consists of a conducting liquid in a curved tubular container. As the unit undergoes tilt, an air bubble moves relative to the excitation electrodes and results in changes in the output signal detected at the pickup electrode. An alternating-current (AC) bridge is necessary since the liquid can be polarized and permanently damaged if a direct-current voltage is applied to the sensor. **B.** The equivalent electrical circuit.

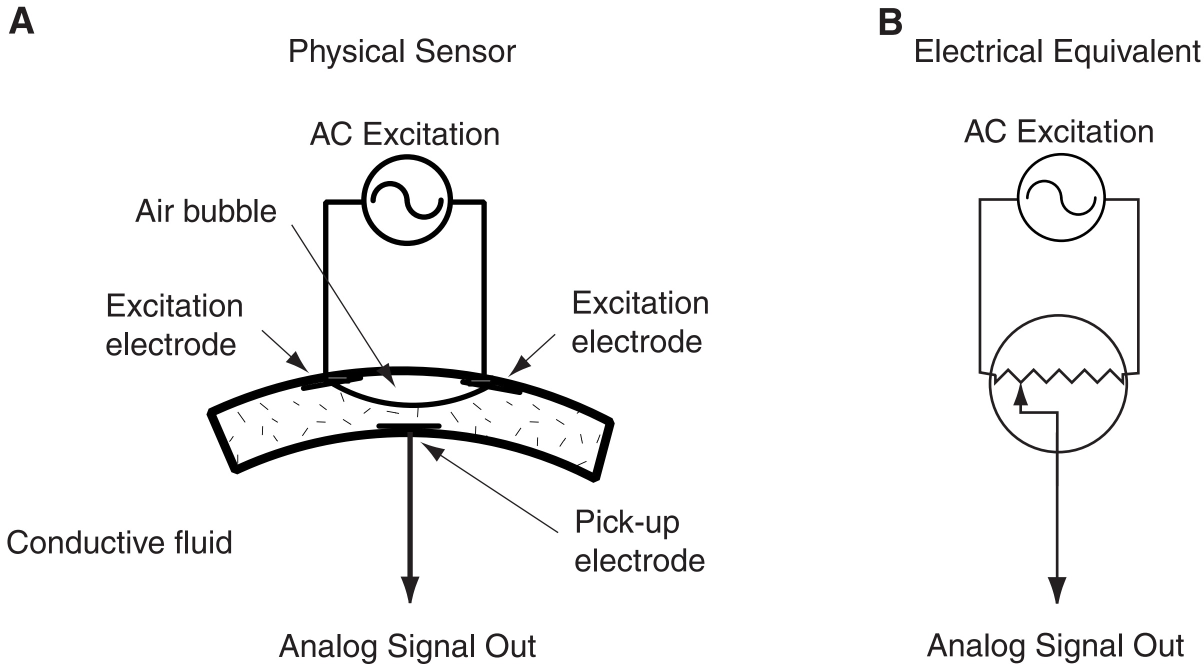

Figure F12. Tiltmeter data from the Nokogiriyama test site. The plot shows ~10 days of data for the two components of tilt. Amplitude scale is given in counts of the 16-bit A/D converter. Tidal tilts are well recorded by this instrument. An earthquake was recorded on 29 April 1999, but our recording rate at that time was inadequate to capture the waveform.

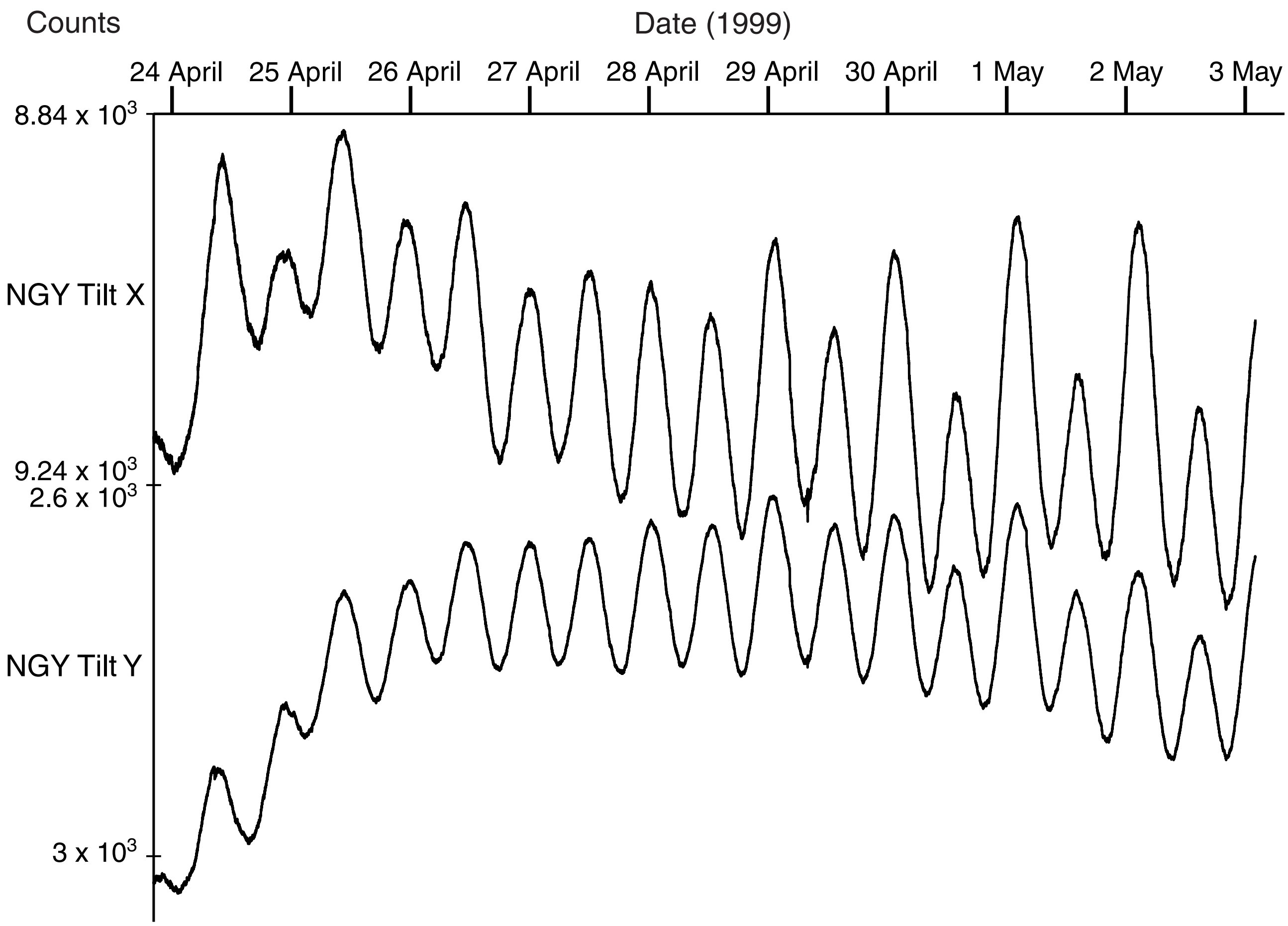

Figure F13. MEG system block diagram. Dashed lines = power distribution; thin lines = serial links; and thick lines = analog signal lines. DC = direct current; SAM = storage acquisition module; SWB = seawater battery; CRM = combiner/repeater module; PDM = power conditioning/distribution module; MOSFET = metal oxide silicon field effect transmitter; OBHS = ocean borehole seismometer; RS = receive/send; TTL = transistor-transistor logic; A/D = analog-to-digital converter; SIM = strainmeter interface module.

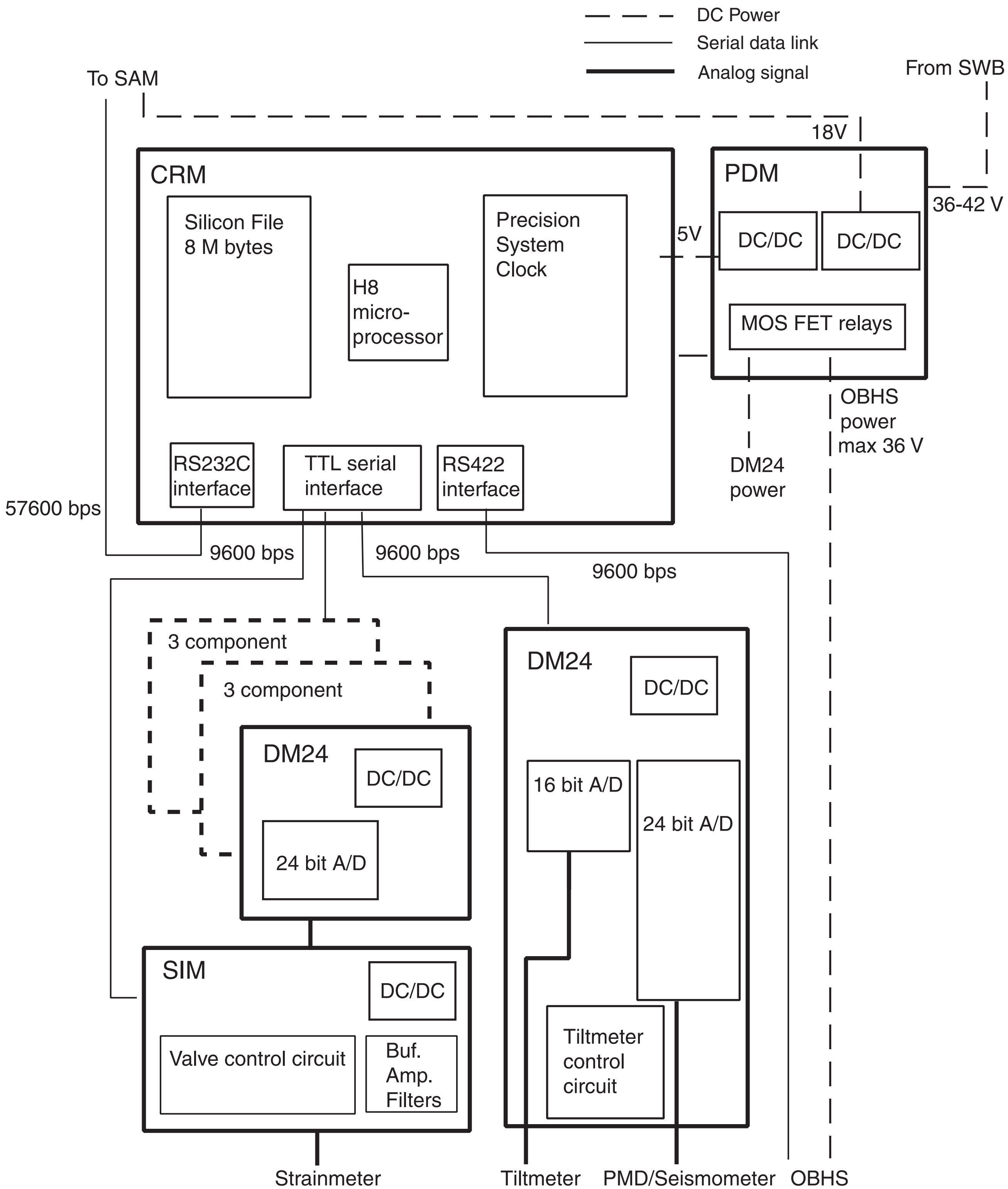

Figure F14. Photograph showing the multiple-access expandable gateway (MEG) canister installed in the MEG frame just before they are sent to the seafloor. ROV = remotely operated vehicle; UMC = underwater mateable connector.

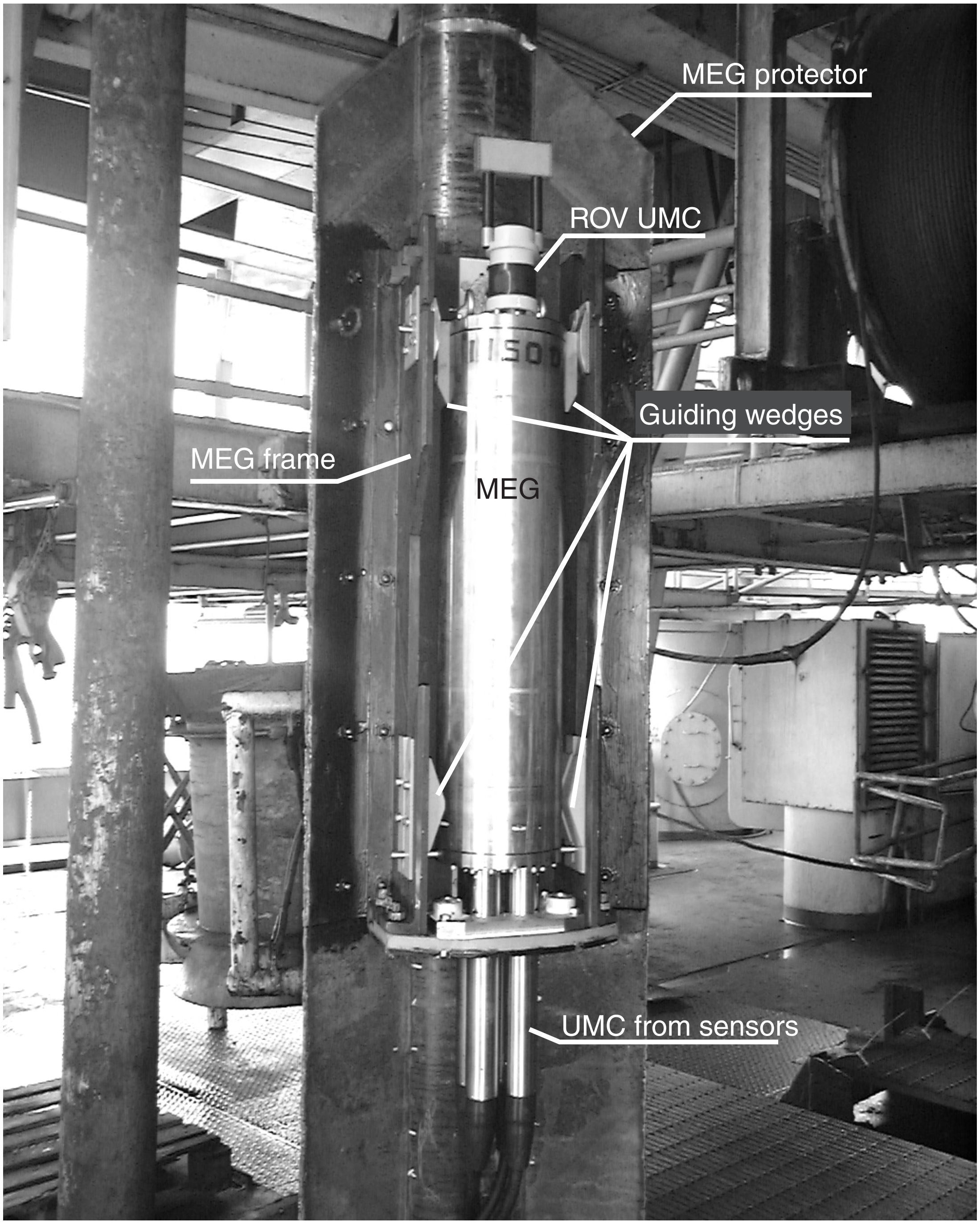

Figure F15. Schematic diagram of the DM24.* A/D = analog-to-digital converter; I/O = input/output; FPGA = field programmable gate array; DSP = digital signal processor; RAM = random access memory; GPS = Global Positioning System; UARTS = universal asynchronous receiver transmitter.

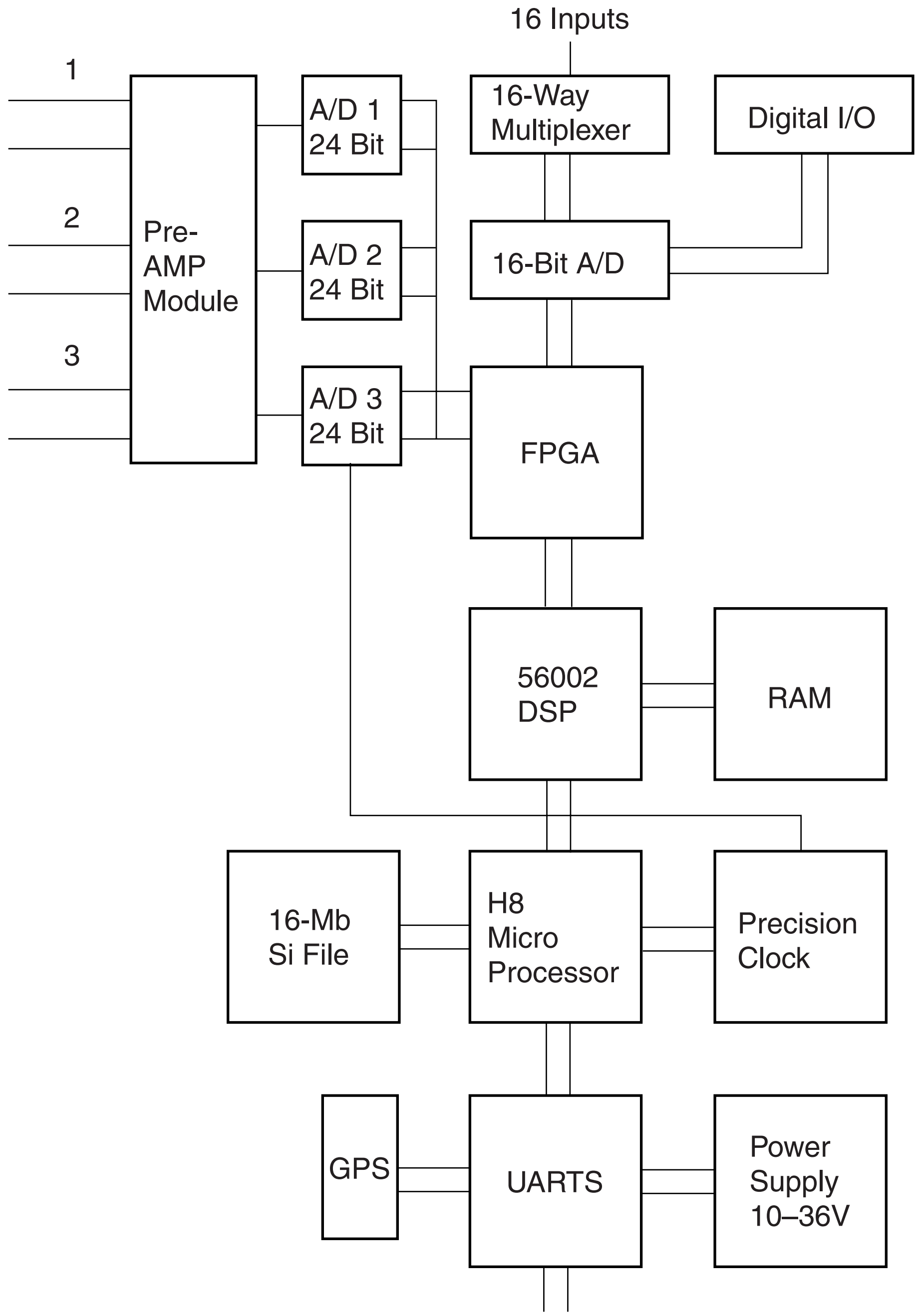

*Reproduced with permission of Guralp Systems Ltd.

Figure F16. Photograph of the SAM unit. The SAM receives the data stream from downhole sensors via the MEG and can store up to 72 GB of data. A replacement SAM module can be installed by an ROV.

Figure F17. Photograph of the BOB to be carried down to the seafloor recorder (SAM) by ROV to check the system status and to collect temporary data. The BOB can be hardwired to the ROV from the port on the BOB's side. Communication is then made via IR interface to the NEREID system.

Figure F18. Results of the system power consumption measurement for the Hole 1151B system. The power supply voltage for the system was 35.4 V. The system was left automatically booting until all the sensors were powered. After the successful start of the whole system, power was shut off temporarily for the PMD seismometer, the tiltmeter, and the corresponding DM24 to evaluate the contribution of the PMD seismometer/tiltmeter components in the consumption. Approximately 4 hr after the system power-up, the system power consumption decreased more than 2 W because of the completion of the charging of NiMH batteries in the storage acquisition module (SAM). OBHS = ocean borehole seismometer; CRM = combiner/repeater module; SIM = strainmeter interface module.

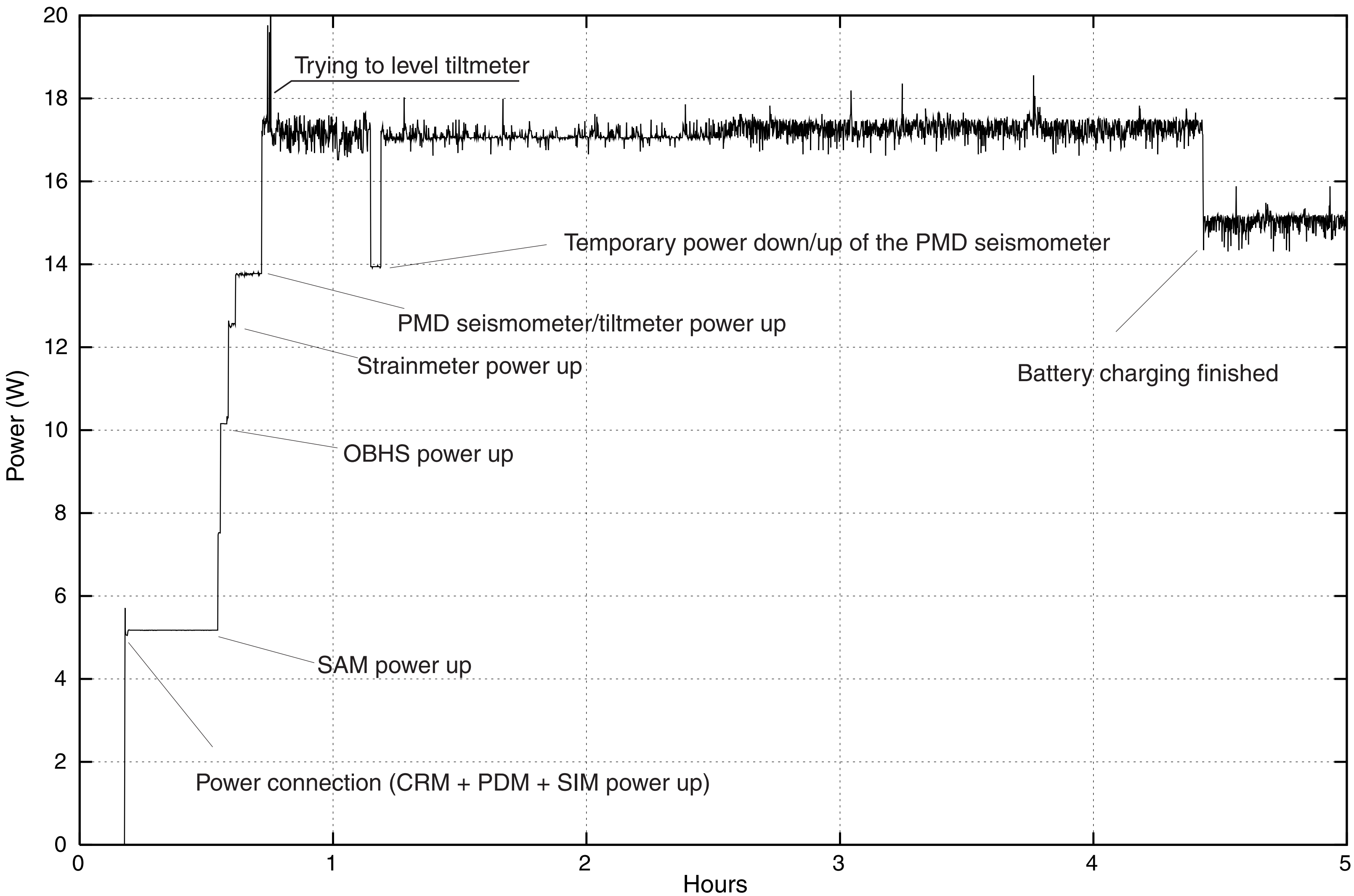

Figure F19. Seawater battery (SWB1200) cell structure.

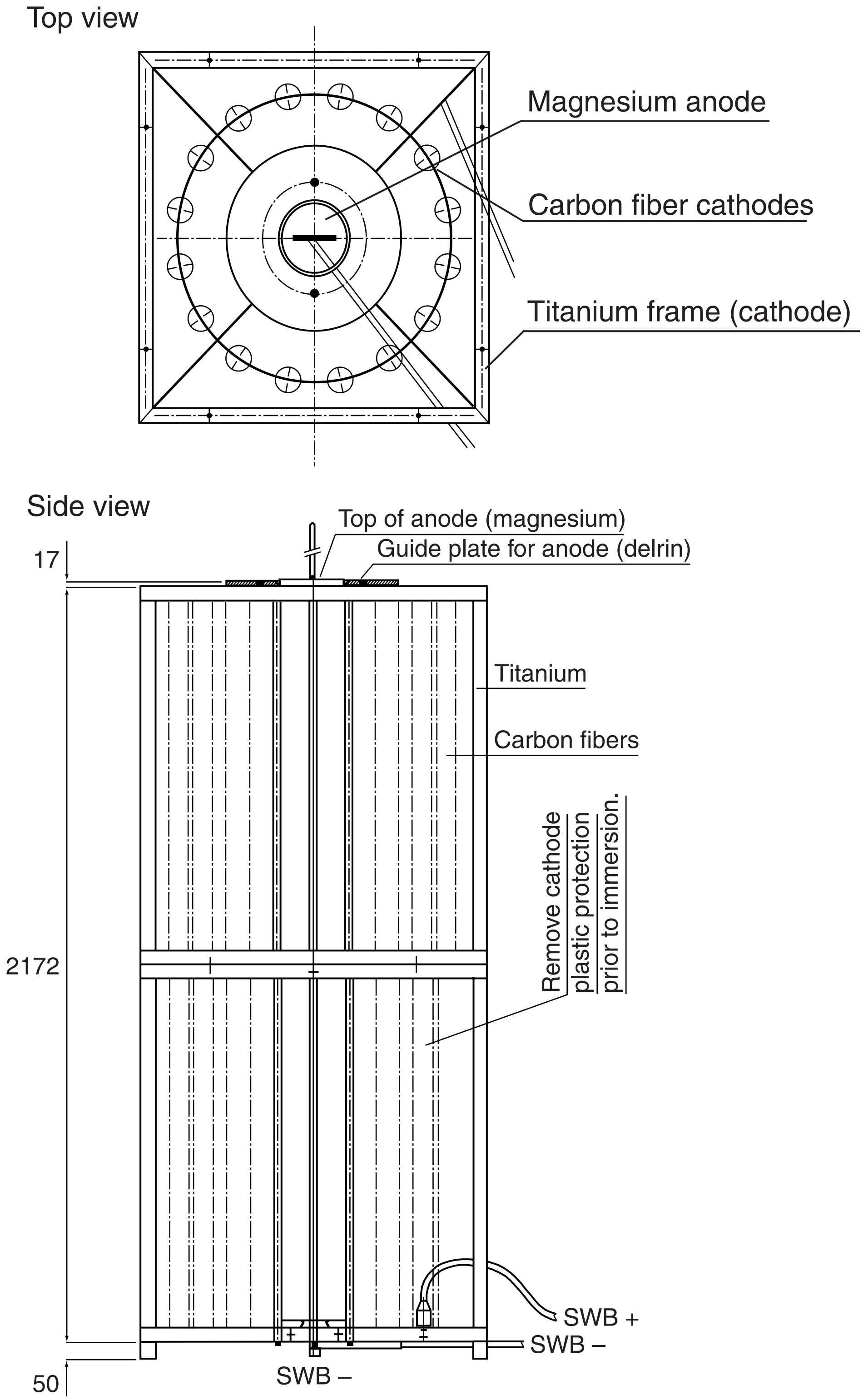

Figure F20. Structure of the carbon fiber brush used in the cell cathode.*

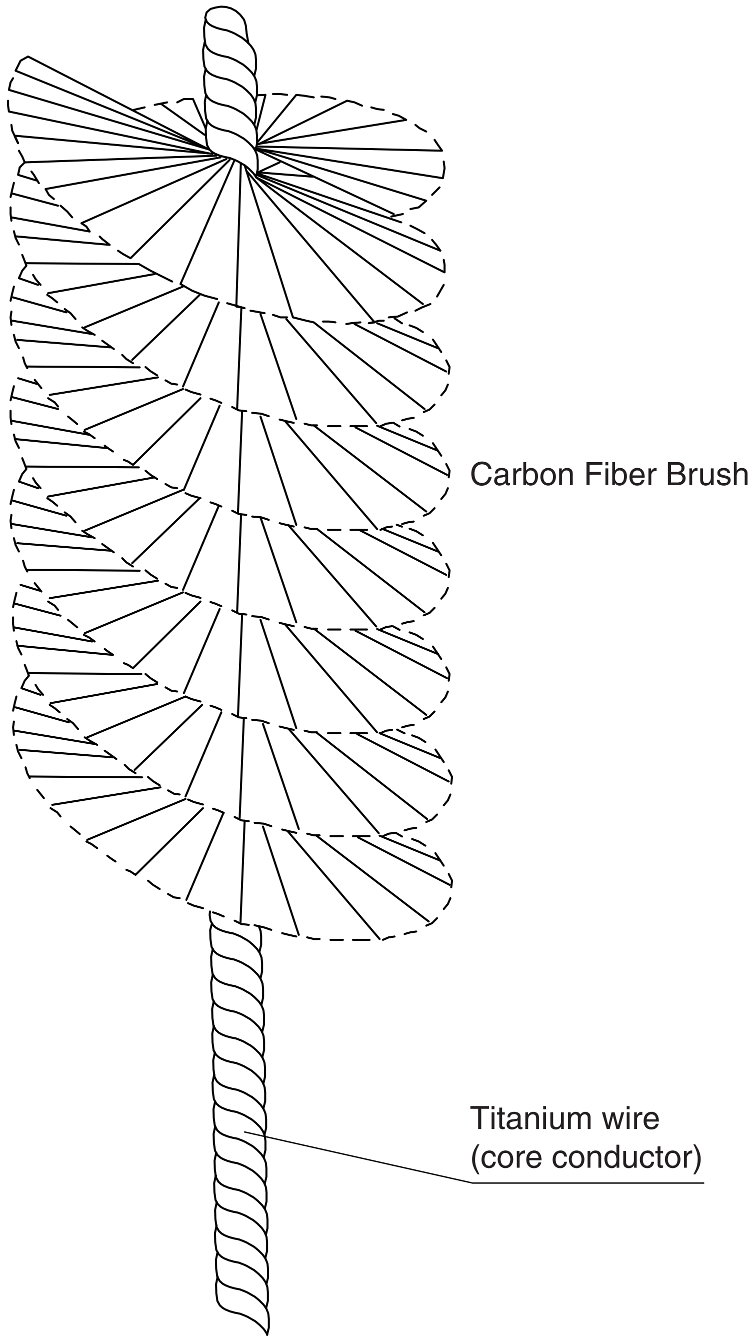

*Reproduced from *J. Power Sources*, Vol. 65, Hasvold, Ø., Henriksen, H., Melvær E., Citi, G., Johensen, B.Ø., Kjønigsen, T., and Galetti, R., Sea-water battery for subsea control systems. pp. 253–261, 1997, with permission of Elsevier Science.

Figure F21. Side-view drawing of power access terminal (PAT) on top of the reentry cone. The riser assembly, also shown in the drawing, extends through the center hole of the PAT. The position of the PAT is defined by the reentry cone and the centralizing rings on the riser assembly located at the bottom of the PAT. MEG = multiple-access expandable gateway.

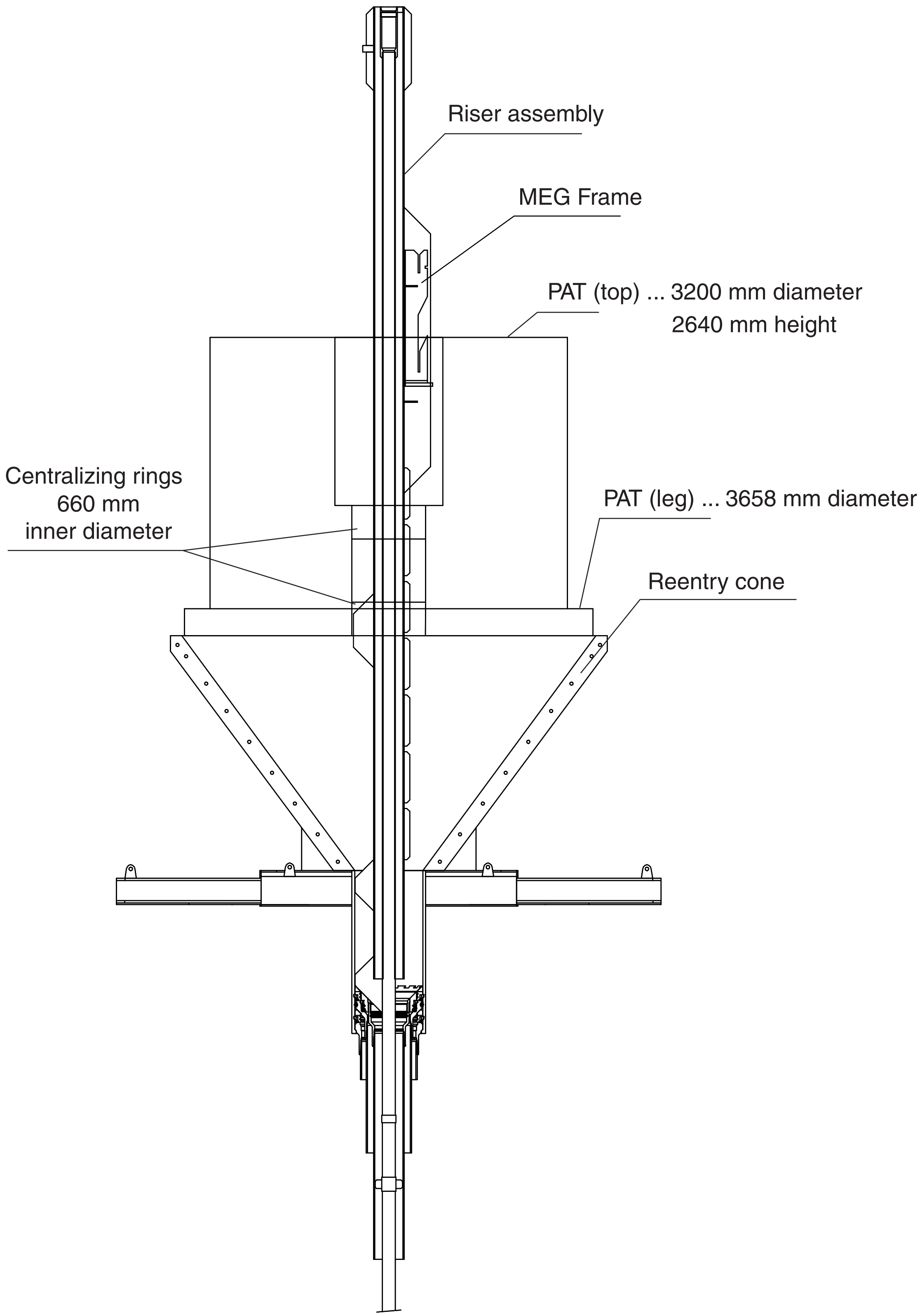

Figure F22. Photograph of the PAT from above the moonpool.

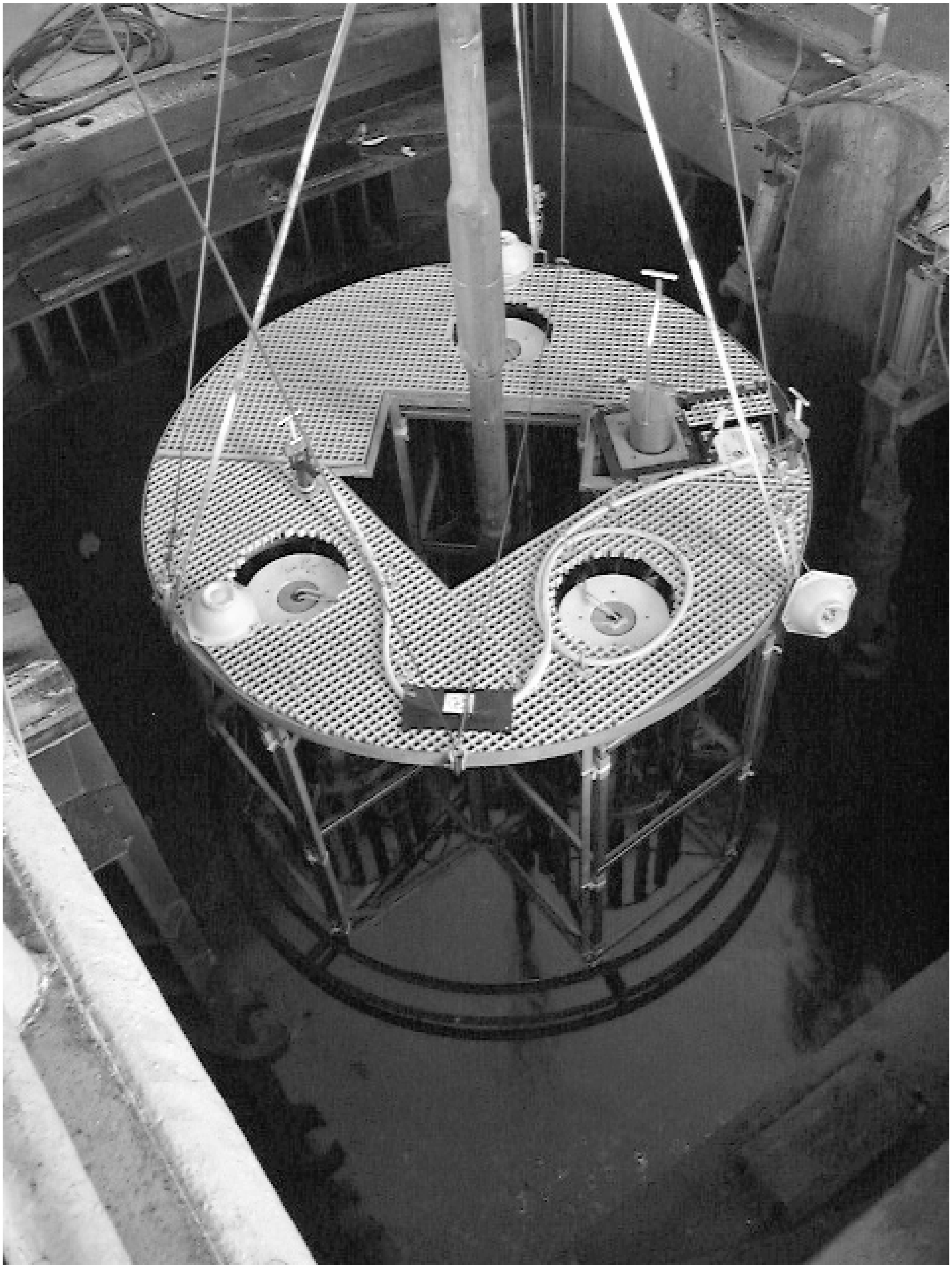

Figure F23. Photograph of the recorder frame with the storage acquisition module (SAM) in place. Co-Chief Kiyoshi Suyehiro is operating the ejecting handle for the SAM, which will be operated by an ROV. UMC = underwater mateable ROV connector.

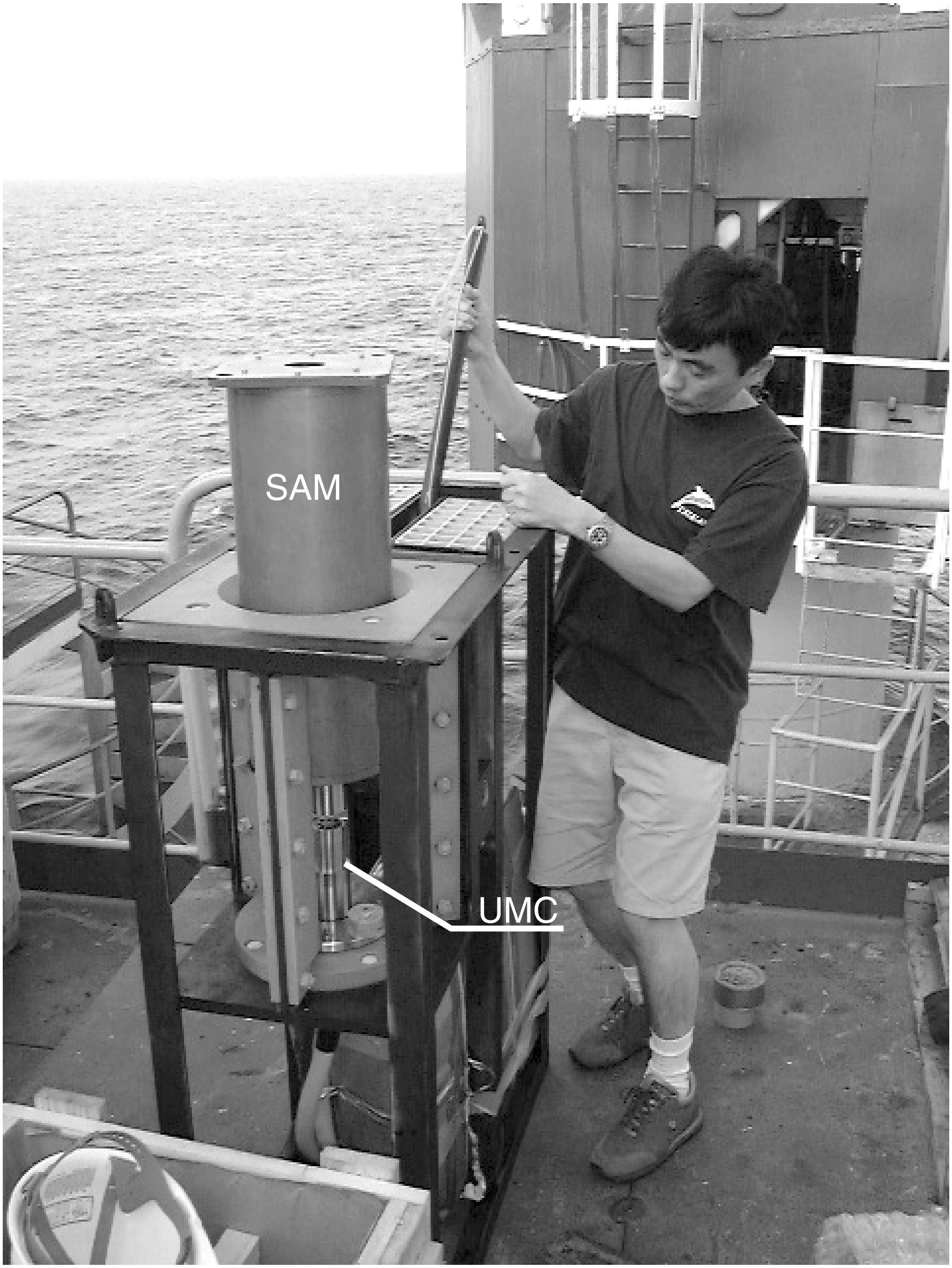

Figure F24. Photograph of the Japan Marine Science and Technology Center (JAMSTEC) ROV, *Dolphin 3K,* which made the first visits to Sites 1150 and 1151 in September 1999. The payload is 150 kg. Manipulators are each 1½ m long and can exert 20 kg force. The shear cutter can cut 50-mm diameter rope. The RS232 port can communicate with NEREID.

Figure F25. Layout of the existing fiber-optic cable system of the University of Tokyo. A cable extension is possible for connecting the NEREID systems. OBS = ocean bottom seismometer; TM = tsunami monitor.

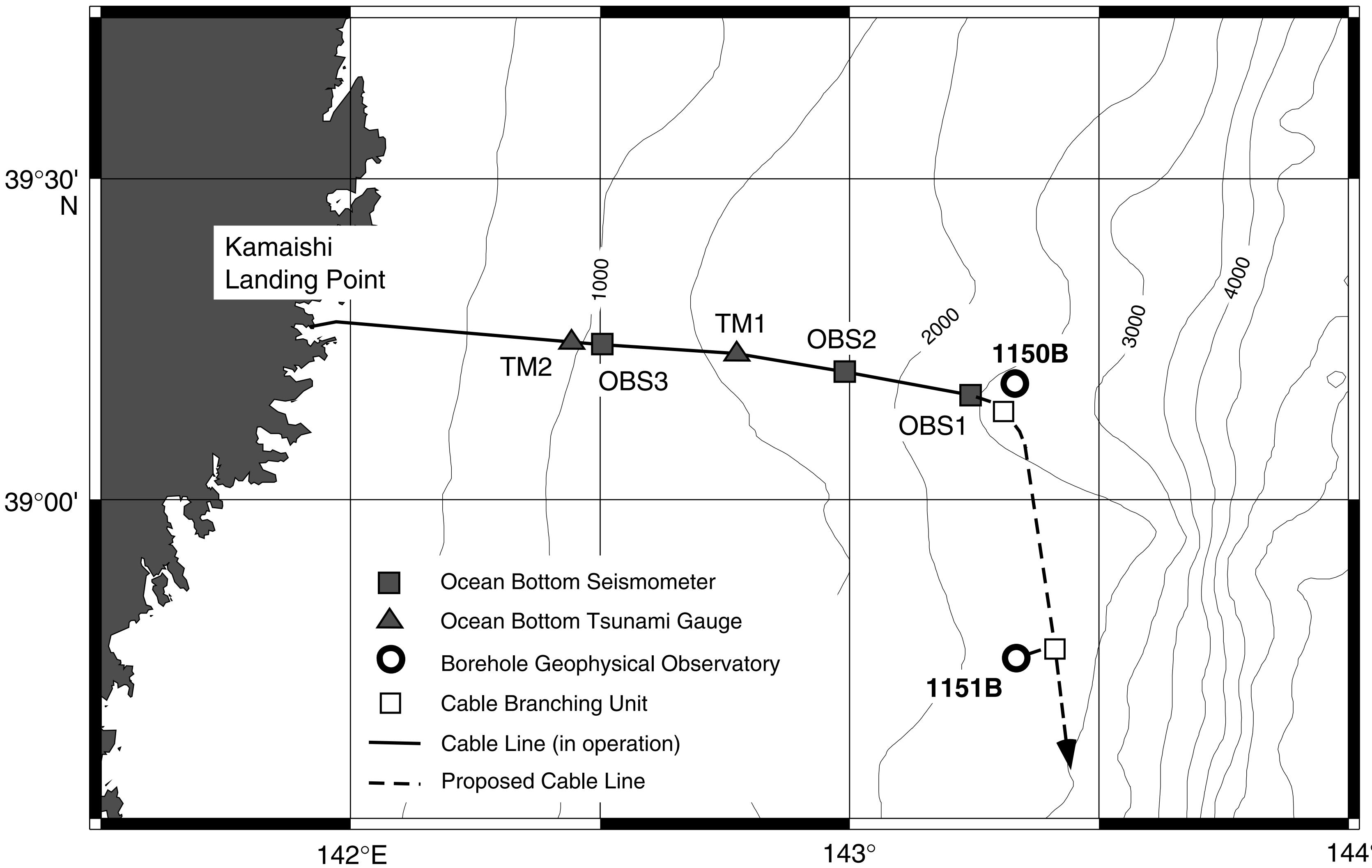

Figure F26. Connection schematics of NEREID systems to the existing fiber-optic cable by use of branching units (BUs). NEREID = 'Neath Seafloor Equipment for Recording Earth's Internal Deformation; MEG = multiple-access expandable gateway.

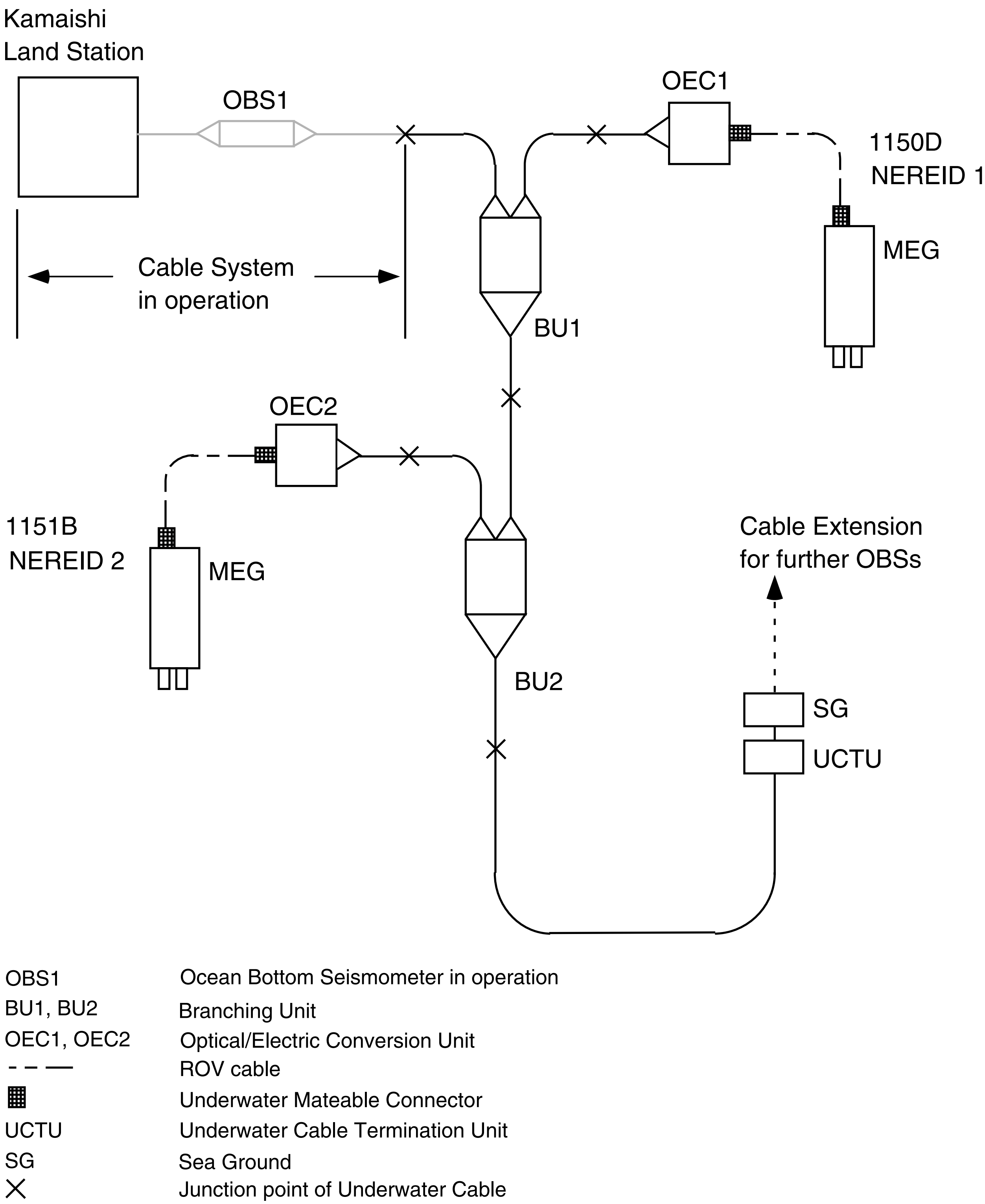

Figure F27. Fiber-optic cable system diagram. ROV = remotely operated vehicle; BU = branching unit; UCTU = underwater cable termination unit; TM = tsunami monitor; OBS = ocean bottom seismometer; OEC = optical/electrical conversion unit; MEG = multiple-access expandable gateway.

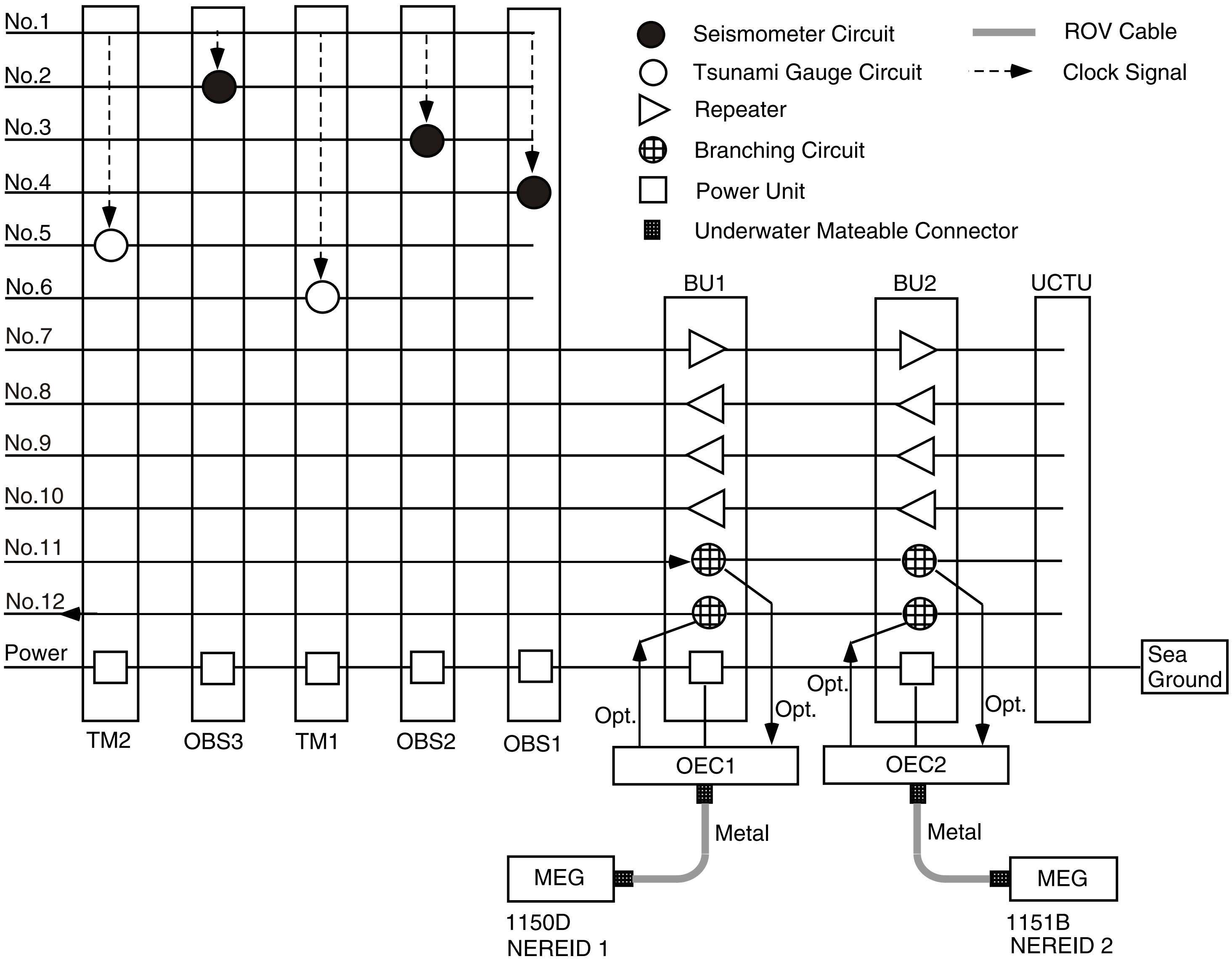

Table T1. Mapping between sensor channels and stream ID in Guralp compressed format.

Sensor channels	Stream ID
Strainmeter DT1 component 1	DTMAZ4
Strainmeter DT1 component 1 high gain	DTMAN4
Strainmeter DT2 component 1	DTMAE4
Strainmeter DT1 component 2	DTMBZ4
Strainmeter DT1 component 2 high gain	DTMBN4
Strainmeter DT2 component 2	DTMBE4
Strainmeter DT1 component 3	DTMCZ4
Strainmeter DT1 component 3 high gain	DTMCZ4
Strainmeter DT2 component 3	DTMCZ4
Tiltmeter x-axis	PMDTM8
Tiltmeter y-axis	PMDTM9
PMD DM24 environment channel	PMDTME
PMD x-axis	PMDTN4
PMD y-axis	PMDTE4
PMD z-axis	PMDTZ4
CMG-1T vertical	1020Z2
CMG-1T horizontal north/south	1020N2
CMG-1T horizontal east/west	1020E2
CMG-1T vertical mass position	1020M8
CMG-1T horizontal north/south mass position	1020M9
CMG-1T horizontal east/west mass position	1020MA
CMG-1T temperature	1020ME

Table T2. Available command set for the CRM, DM24s, SAM, and BOB module.

Commands	Resulting actions
CRM available command set	
ok-1	Enable FORTH vocabulary
.tilt	Tiltmeter output display that figures in the 10-bit range
?dtm	List strainmeter status (power supply voltage measurement)
.bauds	Lists all the settings of baud rate for each serial port
@rtc .rtc	Fetch rtc setting and print rtc
port# baud# baud	To change baud rate
id set-id	Set system's ID
streams?	List all the streams being received with the port numbers
open systemID streamID(head 4characters)	Open a terminal session of foreign system using 'pass-thru'
close	Close the pass-thru terminal session
.ids	Show what instrument currently talking to
In the following commands, $$$ is one of { pmd obh sam tilt dtm1 dtm2 dtm3 }:	
$$$ power-up	
$$$ power-down	
	Power up/down each of the components
	"Tilt" is for tilt motor driving circuit
$$$?power	Query PDM status for the component
.power	Display the voltage and current readings in this order: input volts obh dtm1 dtm2 dtm3 pmd tilt (motors) sam
open1/close1	Open/close valve 1
open2/close2	Open/close valve 2
nn mins-delay	Set the start-up delay to 'nn' min (default is 20 min)
yy mm dd hh mm ss set-rtc	Set RTC clock for time stamp
2 ~protect	Disarm protection of the flash memory
save-cmos	Save CMOS memory in the flash memory (EEPROM)
re-sync on	Resynchronize the clock to the next GPS 1 pps
auto-trim	Estimation of clock oscillator trimming coefficient start
interval on	Disable auto-calibration
complete ?	Shows current status of clock synchronization
watch ?	Shows what type of diagnostic message to print
2 gps-type	Set time reference to Garmin NMEA GPS
3 gps-type	Set time reference to stream sync
h8upload	In boot loader prompt, upload system program from serial data link using 'xs3' PC program
OBH available command set	
day month year d-day	Set deploy date
.d-day	Show deploy date setting
SAM available command set	
.battery	Query battery status
mmm battery-i	Set battery charge current limit to 'mmm' mA
dir	Display directory of the HDD records
chunk?	Check number of memory chip installed (1 chip = 4 MB)
target#?	Show current target HDD
n target	Set current HDD
BOB available command	
send-flash	Begin data transfer stored in the flash file; sending command and closing terminal window prompts the data transfer to begin
.flash	Shows read/write pointer of the flash file that results in an answer such as "writing 0/371... reading ?/?," where 0 = number of chips and 371 = number of blocks

Note: CRM = combiner/repeater module, OBHS = ocean borehole seismometer, SAM = storage acquisition module, BOB = back from ocean bottom module.

Table T3. Pin assignments of Ocean Design underwater mateable stab plate connectors.

	Subcon on sensor	Kintec on sensor	UMC on MEG	DB in MEG	UMC on SAM	DB in SAM	Function
Guralp CMG-1 seismometer and MEG	1	—	1	8	—	—	Power +36V
	2	—	7	9	—	—	Power GND
	3	—	5	9	—	—	Power GND
	4	—	3	5	—	—	Sig-l GND
	5	—	8	3	—	—	Rx(+)
	6	—	6	4	—	—	Rx(–)
	7	—	4	2	—	—	Tx(+)
	8	—	2	1	—	—	Tx(–)
PMD seismometer and MEG	3	—	5	1	—	—	x(+)
	4	—	3	6	—	—	x(–)
	5	—	8	2	—	—	y(+)
	6	—	6	7	—	—	y(–)
	7	—	4	3	—	—	z(+)
	8	—	2	8	—	—	z(–)
	1	—	1	5	—	—	Power (+12V)
	2	—	7	9	—	—	Power GND
Strainmeter (Dil) and MEG (for NEREID-2)	—	15	9	8	—	—	Valve #2(–)
	—	20	12	10	—	—	DT2 out (–)
	—	19	11	9	—	—	DT1 out (–)
	—	13	10	1	—	—	DT1 out (+)
	—	2	8	14	—	—	Valve #1(+)
	—	3	7	7	—	—	Valve #1(–)
	—	4	6	15	—	—	Valve #2 (+)
	—	6	5	5	—	—	DT2 in (+)
	—	10	4	12	—	—	DT2 in (–)
	—	11	3	6	—	—	DT1 in (+)
	—	12	2	13	—	—	DT1 in (–)
	—	14	1	2	—	—	DT2 out (+)
Strainmeter (three-component) and MEG (for NEREID-1)	—	15	9	8	—	—	Valve #1(+)
	—	20	12	10	—	—	Valve #1,2 (–)
	—	19	11	9	—	—	Valve #2 (–)
	—	13	10	1	—	—	DT out (com)
	—	2	8	14	—	—	DT in (+)
	—	3	7	7	—	—	DT in (–)
	—	4	6	15	—	—	DT1a (+)
	—	6	5	5	—	—	DT1b (+)
	—	10	4	12	—	—	DT1c (+)
	—	11	3	6	—	—	DT2a (+)
	—	12	2	13	—	—	DT2b (–)
	—	14	1	2	—	—	DT2c (+)
Tiltmeter and MEG	1	—	9	1	—	—	x out (+)
	2	—	12	9	—	—	x out (–)
	3	—	11	2	—	—	y out (+)
	4	—	10	10	—	—	y out (–)
	5	—	8	4	—	—	Gain 2
	6	—	7	12	—	—	Gain 3
	7	—	6	5	—	—	x motor control
	8	—	5	6	—	—	y motor control
	9	—	4	13	—	—	Motor return
	10	—	3	8	—	—	Power (–12V)
	11	—	2	7	—	—	Power (+12V)
	12	—	1	15	—	—	Power GND
MEG and SAM	—	—	1	3 and 4*	1	3, 4, 5, and 6	Battery GND (0V)
	—	—	2	1 and 2*	2	1 and 2	Battery V+ (36V)
	—	—	3	6†	3	15	GPS 1pps
	—	—	4	2†	4	14	GPS Rx
	—	—	5	7 and 8*	5	7 and 8	SAM power (+18V)
	—	—	6	11*	6	11	Tx data
	—	—	7	12*	7	12	Rx data
	—	—	8	13*	8	13	Sig-l GND

Table T4. Assignment of light-emitting diodes (LEDs) in the system diagnostics matrix display on the BOB module.

LED chart

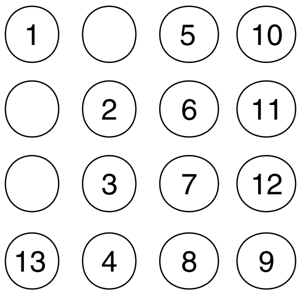

LED NUMBER	FUNCTION	OFF	RED STEADY	RED FLASHING	GREEN STEADY	GREEN FLASHING
1	BOB	fault	fault	SLEEP	fault	ACTIVE
2	MEG	OFF	fault	BOOT STATUS	POWER-UP TIMER	ACTIVE
3	OBHS-CMG1	OFF	LOCKED	UNLOCKING	UNLOCKED	CENTERED
4	OBHS DATA	OFF	POWER ON	BOOT STATUS		DATA BLOCKS
5	DM24-DTM1	OFF	POWER ON	BOOT STATUS		DATA BLOCKS
6	DM24-DTM2	OFF	POWER ON	BOOT STATUS		DATA BLOCKS
7	DM24-DTM2	OFF	POWER ON	BOOT STATUS		DATA BLOCKS
8	DM24-PMD	OFF	POWER ON	BOOT STATUS		DATA BLOCKS
9	TILTMETER	OFF	POWER ON	LEVELING	NOT LEVEL	LEVELED
10	DTM MICRO		fault - no status			STATUS OK
11	VALVE 1	unknown	OPEN		CLOSED	
12	VALVE 2	unknown	OPEN		CLOSED	
13	SAM		BYPASSED		DATA TRANSFER	DISC BACKUP
14						
15						
16						